

9. PRINCIPAL RESULTS¹

Shipboard Scientific Party²

INTRODUCTION

The primary objective for drilling the Côte d'Ivoire-Ghana Transform Margin during ODP Leg 159 was to assess the sedimentary and deformational processes that were operative along this continental borderland as a result of the different stages of continental breakup and related transform tectonism. Comparisons with other passive continental margins (volcanic and nonvolcanic), which also result from continental breakup, indicate that the active transform margin tectonics and subsequent passive development are characterized by (1) a diachronous tectonic history, initially dominated by extensional rifting, followed by transform motion between two plates, and likely recorded by high rates of subaerial to shallow-water sedimentation; (2) a complex history of thermally triggered vertical displacement (uplift and subsidence) due to the proximity (and sharp transition) of a passing, hot, oceanic spreading center; (3) a final stage of sedimentation strongly influenced by the inherited transform structural framework (i.e., the Côte d'Ivoire-Ghana Marginal Ridge and associated features).

Basile et al. (1992, 1993), following Masclé and Blarez (1987), have proposed a four-stage schematic evolution of the Côte d'Ivoire-Ghana Transform Margin. Leg 159 was designed to test this model by evaluation of the timing, the succession of tectonic and thermal regimes, the rates and types of sedimentation, and the degree of sediment diagenesis. These different stages also may be found at other transform-generated margins.

Stage 1. Early Rifting of the Deep Ivorian Basin and Shearing of Its Southern Border (see Fig. 11A of "Introduction" chapter, this volume.)

During Early Cretaceous time, before continental breakup, the African and South American landmasses were in contact along their equatorial boundaries. The future Deep Ivorian Basin and the Ghanaian shelf were facing their Brazilian Margin conjugates, respectively the Barreirinhas Basin and the Piauí-Ceará area.

Between Neocomian and Aptian time, the Deep Ivorian Basin started to rift as a result of an almost east-west oriented extension, generating north-south trending half-grabens and associated rotated blocks. The sedimentary infill (synrift seismic Unit A) probably reached its maximum thickness in half-grabens and along the future transform margin where tectonic features were also generated.

Data from deep dives (Masclé et al., 1993) demonstrate that the sedimentation was chiefly detrital and in subaerial, deltaic, and lacustrine environments. In the future transform area, detrital sedimentation may have been directly influenced by the proximity of the Brazilian Shelf, and potentially controlled by rapid subsidence in pull-apart basins.

Coeval with the extensional basin deepening (due to crustal thinning), shear motion between the continental plates affected the southern border of the African Plate, which evolved as a structural accommodation zone, undergoing concurrently: (a) vertical motion between the extending Deep Ivorian Basin and the adjacent Brazilian platform; and (b) an increase in horizontal (transcurrent) motion from west to east. This resulted in the creation of early en échelon strike-slip fault zones and associated basins generated at the contact between the two domains and in the tilting of the northern slope of the future Marginal Ridge. Near the end of this stage, transform motion shifted toward the south, to the top of the present continental slope where seismic surveys and deep dives show evidence for dextral motion on major faults trending N60°E.

Stage 2. End of Rifting and Intracontinental Transform Faulting (see Fig. 11B of "Introduction" chapter, this volume)

Rifting ceased in the extensional Deep Ivorian Basin when oceanic crust started to be emplaced along its western edge sometime in the Albian. Continental breakup was sealed by a post-rift unconformity and the deposition of seismic Unit B. Along the future Marginal Ridge, initiation of seafloor spreading increased transform-type displacement between the two continental borderlands.

Stage 3. Continent/Ocean Transform Faulting (see Fig. 11C of "Introduction" chapter, this volume)

In Santonian time, final continental separation between West Africa and northeast Brazil brought into contact the newly created Gulf of Guinea oceanic crust and the continental transform, which then became an active continental transform margin. Tectonic activity is thought to have shifted from a broad continental wrench zone to a narrower fracture zone within the thin and weaker oceanic crust. Differences in depth between the continental border and the oceanic basin would have led to gravitational sliding, progressive creation of the steep southern slope of the Marginal Ridge, and exhumation of early synrift units.

The contact between hot oceanic lithosphere and colder continental crust is expected to have induced strong thermal gradients and resulted in subsequent Marginal Ridge uplift during the Late Cretaceous. Within the adjacent Deep Ivorian Basin, coeval sedimentation is believed to have recorded such an uplift, while the preexisting sedimentary units were tilted northward. This uplift probably increased until the passage of the oceanic spreading ridge; it also may have been recorded by mineral transformations and a strong phase of erosion, especially along the ridge crest.

Stage 4. Passive Margin Evolution (see Fig. 11D of "Introduction" chapter, this volume)

Active tectonism along the transform margin ceased when the spreading center passed southwest of the Côte d'Ivoire-Ghana Margin. The transform margin and the adjacent oceanic basin then started to subside as a result of lithospheric cooling. Subsequently, the strong

¹Masclé, J., Lohmann, G.P., Clift, P.D., et al., 1996. *Proc. ODP, Init. Repts.*, 159: College Station, TX (Ocean Drilling Program).

²Shipboard Scientific Party is given in the list preceding the Table of Contents.

damming effect of the Marginal Ridge restricted most of the detrital sediment input to the Deep Ivorian Basin.

The interpretation of the local structural and paleogeographic evolution may be considered in the broader context of the rifting of the Central and South Atlantic basins. Figure 1 shows a series of plate tectonic maps taken from the program *Terra Mobilis* (1988). This reconstruction draws on seafloor spreading anomalies and paleomagnetic data from the South American and African cratons to constrain the timing of breakup. Although the rate of spreading is poorly known in this part of the equatorial Atlantic due to the low latitudes and the middle Cretaceous magnetic quiet zone, the spreading history is better constrained farther north and south. This reconstruction implies that during Albian times, seafloor spreading had started in the southern South Atlantic, but that in the Côte d'Ivoire-Ghana region the continents were still in contact, although rifting and strike-slip deformation were in progress. Reconstruction for the Turonian suggests that during this time the spreading ridge, south of the Romanche Fracture Zone, was migrating along the present Côte d'Ivoire-Ghana Marginal Ridge. Finally, a reconstruction for the late Paleocene shows that, at this time, the equatorial Atlantic was a fully open seaway and the Côte d'Ivoire-Ghana Margin had become passive. This may be significant in the interpretation of the major unconformities of this age that were observed at Sites 960–962. Deformation during this time span might therefore be expected to reflect passive margin subsidence following rifting and thermal relaxation after passage of the oceanic spreading center.

SEDIMENTARY FACIES, STRUCTURAL DEFORMATION, AND PALEOGEOGRAPHIC EVOLUTION

The interplay of tectonic deformation and sedimentation on the Côte d'Ivoire-Ghana Transform Margin is best represented in the

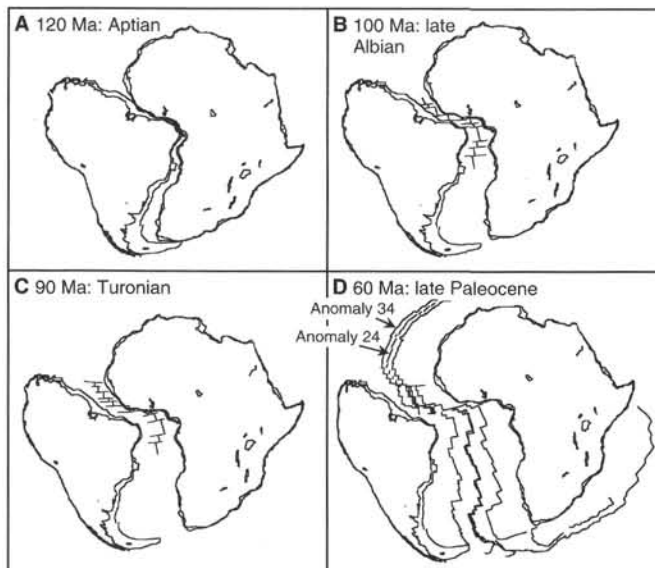


Figure 1. A–D. Simplified spreading model for the Central and South Atlantic basins derived from paleomagnetic data from South America and Africa, as well as available seafloor spreading anomalies (anomalies 24 and 34 are delineated). Reconstruction is from *Terra Mobilis* (1988). Note that seafloor spreading began during the Aptian in the southern Atlantic but that the Côte d'Ivoire-Ghana region was clearly an area of continent-continent transform tectonics until the Albian. A Turonian age is most probable for the passage of the ridge crest along the Côte d'Ivoire-Ghana Marginal Ridge.

spatial and stratigraphic variation of sediments cored at Sites 959 and 960. Although important information is provided by cores from Sites 961 and 962, the completeness of these sections, and thus the direct contribution for interpreting paleoenvironmental settings, is comparatively limited. The most striking feature common to all localities is the prevalence of hiatuses throughout the section. Using the sedimentary facies data, only short periods of time can be reconstructed on a regional scale. This is due to a variety of reasons including difficulties in recovery, the possible removal by erosion or slumping of thick intervals of sediment, and periods of nondeposition. As a result, we have focused on the comparatively complete records provided by Sites 960 and 959 to reconstruct paleoenvironmental conditions that prevailed from late Albian through Holocene times on the Côte d'Ivoire-Ghana Marginal Ridge and adjacent Deep Ivorian Basin.

On the basis of sections reconstructed for Sites 959 and 960 (Figs. 2, 3), three principal stages have been identified that mark changes in the paleoenvironmental setting: I. Intra-continental to Syntransform Basin Stage; II. Marginal Ridge Emergence Stage; and III. Passive

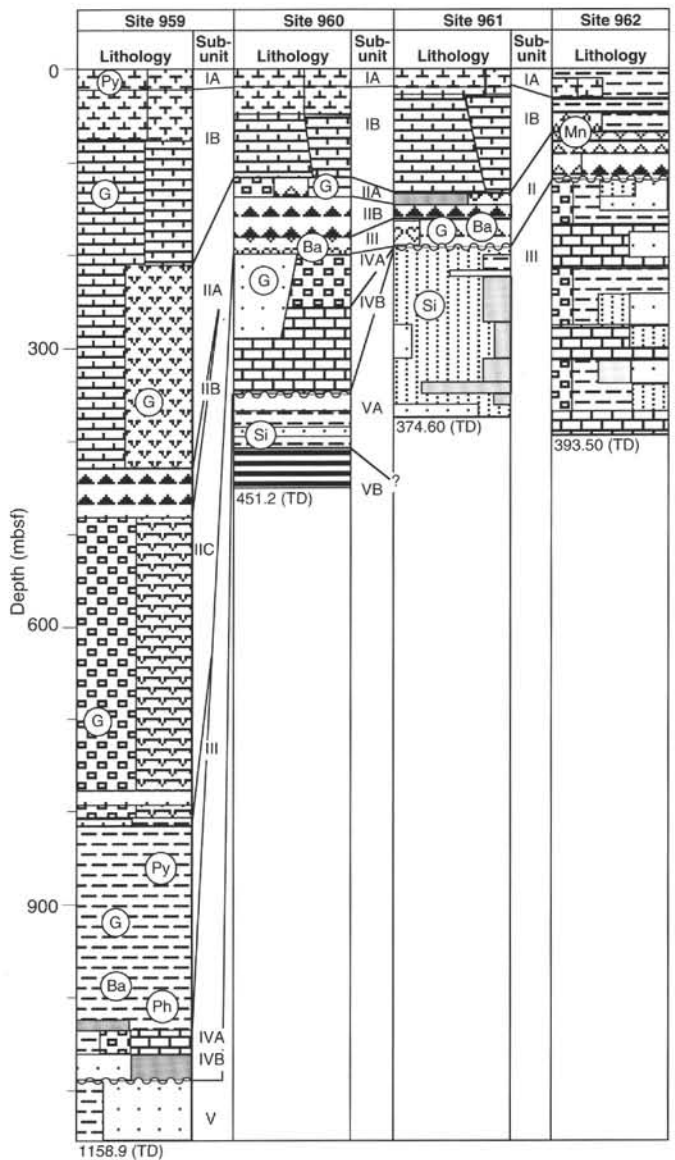


Figure 2. Lithostratigraphic columns for all four sites showing the variation in thickness of the different units between sites. See "Explanatory Notes" chapter (this volume) for key to lithologies.

I. Syntransform Basin Stage

Depositional Environment: Temporal and Spatial Changes

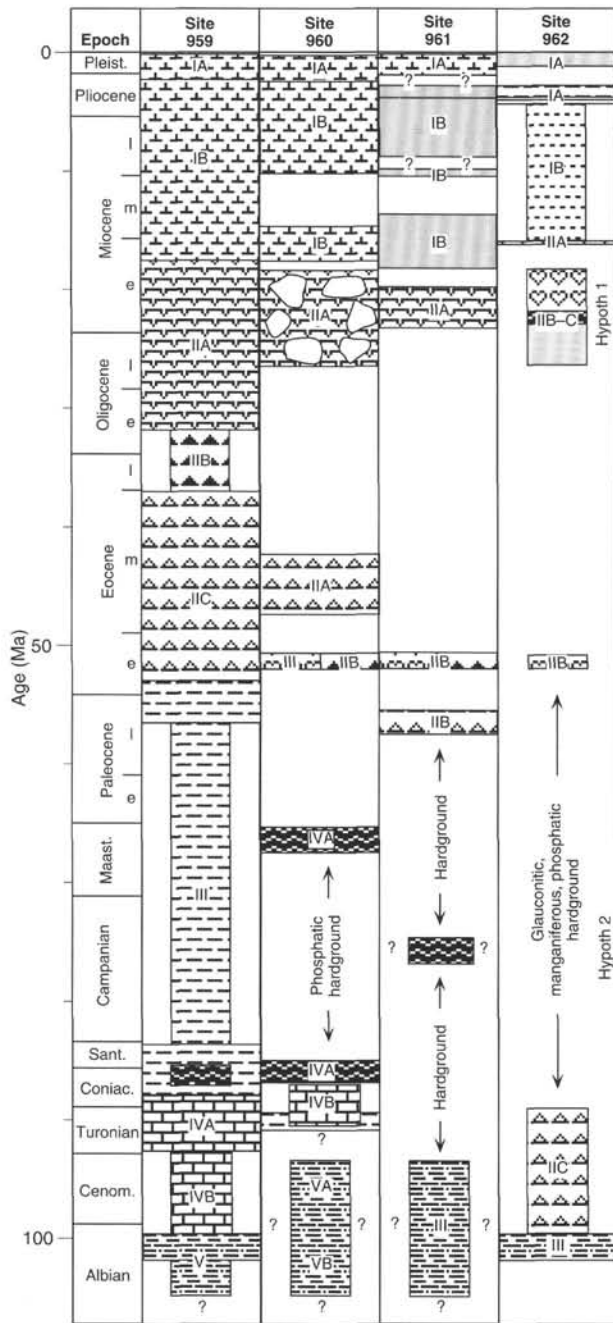


Figure 3. Chronostratigraphic diagram showing the variation in sedimentary facies between sites at different times since the inception of continental breakup. Note common period of hiatus and/or condensed sedimentation during the Paleocene and Late Cretaceous, and during the Oligocene and late Eocene at Sites 960–962.

Margin Stage, which is subdivided into intervals of Basin and Ridge Differentiation, Biosiliceous Sedimentation, and Carbonate Pelagic and Hemipelagic Sedimentation. These stages reflect lithologically distinct intervals in the sedimentation history and relate to changes in the tectonic setting and oceanographic conditions. Even though all of these stages are not present in sediments of Sites 961 and 962, some intervals can be recognized at all sites, and the significance of their spatial relations is discussed below.

The earliest record of sedimentation recovered during Leg 159 is of Albian siliciclastic sequences, which are believed to have formed in deep, tectonically generated basins (probably pull-apart; cf. Crowell, 1974) associated with the transform motion between South America and Africa (Figs. 4, 5). This region is characterized by a progression, both spatially and temporally, from intra-continental basins comprising lacustrine sediments, to marine basins comprising both mixed siliciclastic and pelagic sediments. The transition between these two end-member settings is reflected in sequences that contain abundant medium-grain-sized siliciclastics, which lack marine planktonic and benthic fossils but contain abundant disseminated pyrite, an indication of marine water at the depositional site. This phase of sedimentation is terminated by uplift and associated deformation. Structural inversion is indicated by the transformation of the depositional basin into the uplifted block that presently defines the Marginal Ridge and southern border of the Deep Ivorian Basin.

Three end-member facies are recognized within the syntransform sequence, namely lacustrine, transitional marine, and open marine facies. Most record relatively deep-water settings where sedimentation is characterized by gravity-driven depositional processes, typically below the effective wave base. Thus, changes in the environment from nonmarine to marine have been recognized principally by the presence or absence of marine faunas and of pyrite. For example, the absence of authigenic pyrite and the presence of siderite in organic- and reducible iron-rich sediments is used as a prime indicator for a nonmarine environment. Conversely, the presence of disseminated pyrite and of pelagic faunas, nannofossils and foraminifers is taken as evidence for normal marine salinities and depositional conditions.

Lacustrine sediments recovered from Site 960, lithologic Subunit VB, comprise a thick succession of finely laminated, siliciclastic rhythmites ranging from silty sandstones to silty claystone. These contain abundant plant debris concentrated within the finer sediment fractions (i.e., silty claystones). Siderite is present, occurring as nodules or as finely disseminated cement. Pyrite is absent except in mineralized tectonic fractures. Independent of the inferred salinities of the depositional waters, the sediment character suggests deposition by gravity-driven processes such as density flows into the deeper portions of the basin (Fig. 4). Deep, relatively sediment-starved pull-apart basins are well known in transform settings (e.g., Gulf of Aqaba; Ben-Avraham et al., 1979), even when the basin concerned is relatively narrow (Pitman and Andrews, 1985). In the upper part of this sequence, these grade into coarser grained sandstones that contain pyrite but lack marine faunas or floras. We interpret this sequence as representing the transition from deep lacustrine environments to shallower and more proximal brackish water environments. This transition may record the progressive encroachment of marine conditions during late Albian time.

A similar trend toward more marine conditions is observed in a westward traverse from Site 960 to 962. The basal sequence recovered at Site 961 (lithologic Unit III) comprises a thick interval of silty sandstones to silty claystones that contains abundant disseminated pyrite. This siliciclastic sequence is dominated by quartz and detrital feldspar. Metamorphic quartz is indicated by both strained and composite grains; a coeval igneous source terrane is suggested by the occurrence of minor rutiled quartz, tourmaline, and zircon. Chlorite, though present throughout this section, is interpreted to be of diagenetic origin, in response to burial, tectonic deformation, and thermal maturation (see below). The co-occurrence of angular quartz and feldspar with well-rounded quartz grains suggests multiple sources for detrital sediment. The source of texturally and compositionally mature grains may include coeval shoreface environments, or recycled sediments that had been locally uplifted during transform deformation. However, if this were the case, then these must have been in-

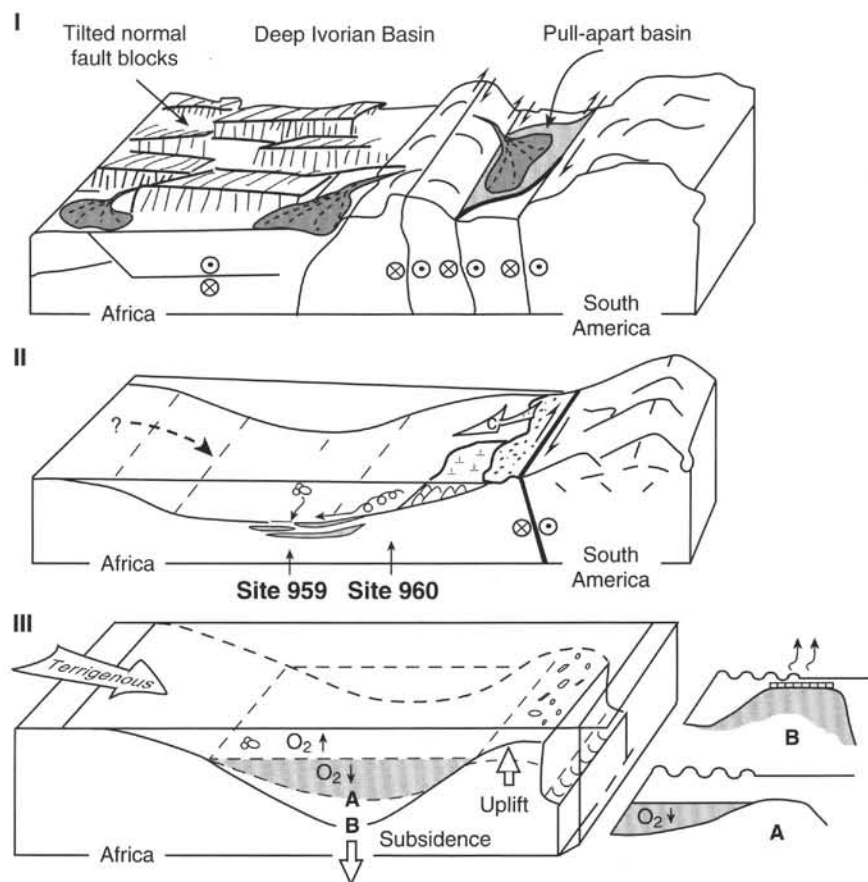


Figure 4. Paleogeographic cartoon depicting the early evolution of the Deep Ivorian Basin and Marginal Ridge (Late Cretaceous to early Eocene). **I.** Syntransform, intracontinental basin stage (unknown to late Albian). The early history of this region is dominated by intracontinental pull-apart basins formed in response to transcurrent shear between the Brazilian and western African cratonic blocks. Sedimentation during the late Albian was dominated by continental and lacustrine environments (Site 959, lithologic Unit V) and transitional marine environments (Site 960, lithologic Unit V; and Sites 961 and 962, lithologic Unit III). **II.** Marginal Ridge emergence, (late Albian to Coniacian). The intercalation of limestone debris and grain flow deposits containing coarse siliciclastic detrital grains with pelagic limestones marks the emergence of the Marginal Ridge and initiation of subsidence in the Deep Ivorian Basin. The emergent ridge provided the source of coarse igneous and metamorphic siliciclastic grains. During this time, the margins of the emergent ridge were colonized by shallow marine reefal complexes, and dominant sediment transport was northward toward the Deep Ivorian Basin (lithologic Subunits IVA, B, Site 959; lithologic Subunit IVB, Site 960). **III.** Submergence of the Marginal Ridge and development of the Deep Ivorian Basin (late Coniacian to early Eocene). **A.** Initiation of dysaerobic Deep Ivorian Basin and hardground formation on the Marginal Ridge (late Coniacian to late Paleocene). Formation of hardgrounds at Sites 959 and 960 (lithologic Subunit IVA) and 961 (lithologic Subunit IIB) marks the cessation of reef development and submergence of the Marginal Ridge. Deposition of a thick sequence of black claystones reflects the initiation of dysaerobic bottom water conditions within the deepening axis of the Ivorian Basin (Santonian to late Paleocene; lithologic Unit III, Site 959). **B.** Differentiation of the Marginal Ridge and Deep Ivorian Basin (late Paleocene to early Eocene). The Deep Ivorian Basin shifted to aerobic bottom water conditions with the deposition of calcareous and biosiliceous pelagic sediments (Site 959, lithologic Subunit IIC). In contrast, the Marginal Ridge is characterized by the formation of palygorskite claystones (Site 960, lithologic Unit III; Site 961 and 962, lithologic Subunit IIB). The genetic significance of palygorskite clay formation is problematic and may reflect either renewed shallowing of the Marginal Ridge and the development of elevated salinity conditions, a period of eolian transport from coastal settings, or formation under deep bottom water conditions. Circled x's and circled dots represent inward and outward relative motion, respectively.

termixed during or prior to transport, as the sedimentary structures do not suggest a shallow-water shoreface setting. At Site 961 sandstones and siltstones with lenticular bedding and isolated ripples are draped by finer claystones and laminated siltstones to claystones. Locally, these structures have been disrupted by burrows, suggesting an active benthic fauna. Replacement of many of these burrows by siderite and the development of nodules is common in a brackish to marine water environment. These observations, and the lack of features associated with turbidity currents, are compatible with a deep, transitional marine setting where the sediment was periodically winnowed by storm-generated waves or bottom currents.

The sedimentary succession at Site 962, farther to the west, records a deep marine depositional setting. Here, a thick sequence of

upper Albian sandstones, siltstones, and claystones is interbedded with varying amounts of nanofossil and micritic carbonate. These lithologies occur in well-developed fining-upward sequences, some of which possess scoured bases, size grading, and upper beds showing parallel and rippled laminations, all indicative of sedimentation from turbidity currents. These, in turn, are locally overlain by laminated sediment enriched in nanofossils. Coarse-grained intervals comprise quartz siltstones and sandstones, or carbonates consisting of benthic and planktonic foraminifers, and rare peloids and bivalve fragments. Fine-grained intervals comprise clays with varying amounts of intermixed nanofossils or quartz silt. Authigenic dolomite and pyrite are abundant within these fine-grained lithologies, perhaps reflecting the concentration of organic material in these sed-

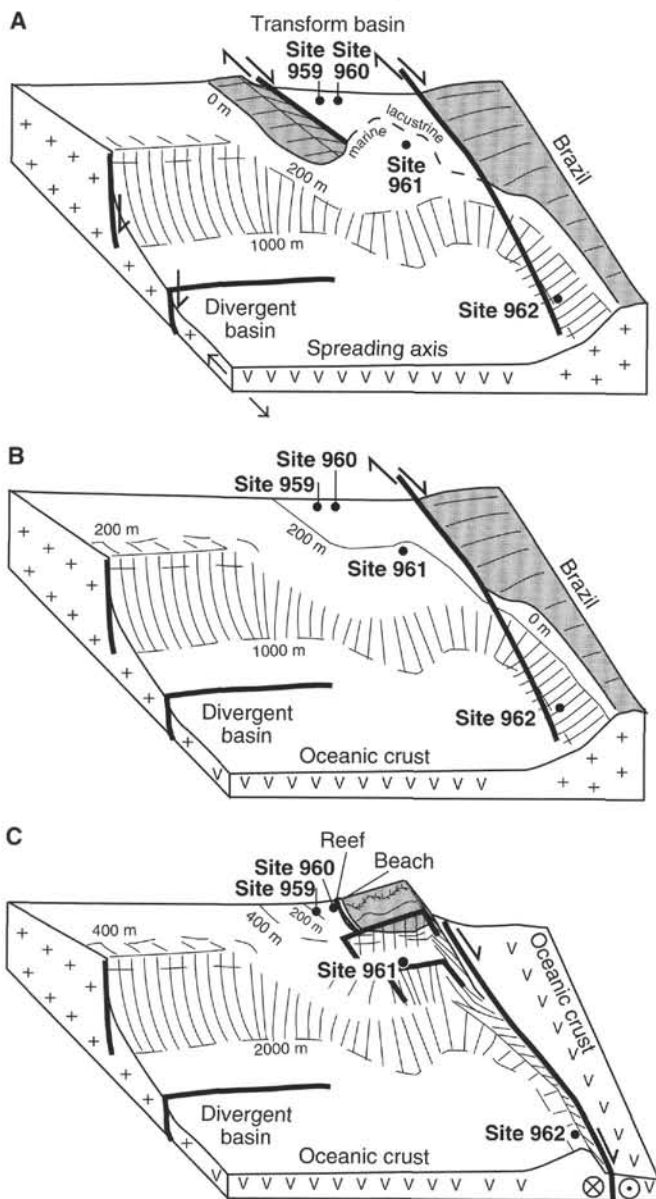


Figure 5. Paleogeographic and tectonic reconstruction of the Côte d'Ivoire-Ghana Marginal Ridge, viewed from the northwest. **A.** Albian. The end of divergent rifting in the Deep Ivorian Basin, with sedimentation and deformation being recorded at Sites 960 and 961. **B.** Late Albian. Early post-rift stage, marked by continued sedimentation and deformation at Sites 959 and 962. Record is missing at Sites 960 and 961, possibly due to later erosion. **C.** Cenomanian-Turonian. Continent/ocean transform stage.

iments. Overall, lithologic Unit III at Site 962 reflects a site of high sedimentation rates, with possibly more than 300 m of sediment accumulation during late Albian time.

Siliciclastic Sediment Sources

Comparison of syntransform sediments between sites indicates that a spectrum of environments, from lacustrine to open marine, may have existed coevally during late Albian time. However, the chronostratigraphy is not well constrained, with the only definitive age derived from Site 962 (see "Biostratigraphy" section, "Site 962" chapter, this volume). In other cases, age control comes from units that overlie an erosional contact. As such, the contemporaneity of conti-

ental and marine depositional environments cannot be unequivocally demonstrated. This has some bearing on the inferred source of the thick succession of siliciclastic sediments. Three possibilities exist: highlands associated with the South American and African continents (or associated tectonic slivers of continental crust along the transform fault complex); recycling of the Marginal Ridge itself; or a combination of both sources.

Clearly, the primary sediment that filled the syntransform basins was derived from uplifted crystalline igneous and metamorphic terranes of continental origin. Recycling of previously deposited, syntransform sediments could occur through structural inversion, a phenomenon envisioned for the region of the present Marginal Ridge. At Site 960, an erosional and angular unconformity is developed between tectonically deformed, pre-Cenomanian siliciclastic sediments and overlying undeformed, Cenomanian to Coniacian carbonates. This implies that erosion of this surface must have been matched by deposition of recycled siliciclastics in adjacent basins. However, with regard to the sediment recovered along the Marginal Ridge, the textural and mineralogical immaturity argues against recycled sediment as a significant contributor to sedimentation.

Timing of Structural Deformation and Uplift of the Marginal Ridge

Deformation of the Albian siliciclastic sequence and uplift of the Marginal Ridge occurred during the latest Albian to early Turonian. Pelagic and periplatform carbonate debris and grain flows unconformably overlie syntransform siliciclastic sediments at Sites 959 and 960, with the transgressing sediment dated as middle Turonian and early Turonian, respectively. This contact represents an angular and erosional contact at both sites. Biostratigraphic control on the uplift is less well constrained at the other sites (Site 961, pre-late Paleocene; Site 962, late Albian to early Miocene). Tectonic deformation below the unconformity is indicated by an abundance of both compressional and extensional structures (slickensides, reverse faults, normal faults, fractures). Fractures associated with such deformation are commonly mineralized with calcite, barite, pyrite, or kaolinite.

The tectonic deformation and structural inversion observed in the syntransform basins could correspond to the decoupling of the South American and African continents (Masle and Blarez, 1987). A relaxation of tectonic stresses along the continent-continent transform could be manifested in the uplift of segments of the transform margin. At present, the southern boundary of this structural block represents the abrupt transition from continental to oceanic crust.

Tectonic Records

The cores from all sites have a range of deformation styles, summarized in Figure 6. Although sediments from many different stratigraphic levels may show deformation, it is noteworthy that the most intense concentration of faults, veins, and microfolds is found toward the base of each site. An abrupt downhole increase in deformation is noted at each site, coinciding with an unconformity between Lower Cretaceous clastic sediments (seismic Unit A) and overlying late Albian-Turonian carbonates at Sites 959 and 960. At Site 961 the age of the overlying sediments is poorly constrained as Cretaceous, whereas at Site 962 the break in deformational intensity appears to be within the upper Albian, at the start of porcellanite sedimentation. These lower intervals of strong deformation are attributed to deformation during the syntransform phase.

The effects of the deformation can be seen in the variation in downhole index properties (Fig. 7). For example, at Sites 960-962 a major break in the porosity values is seen between the tectonized Lower Cretaceous sediments of seismic Unit A, a trend also reflected in the *P*-wave velocity. At each of these sites, the presence of a major unconformity between Cretaceous and Cenozoic is marked by an offset in the porosity data. At Sites 961-962 the change is noted between

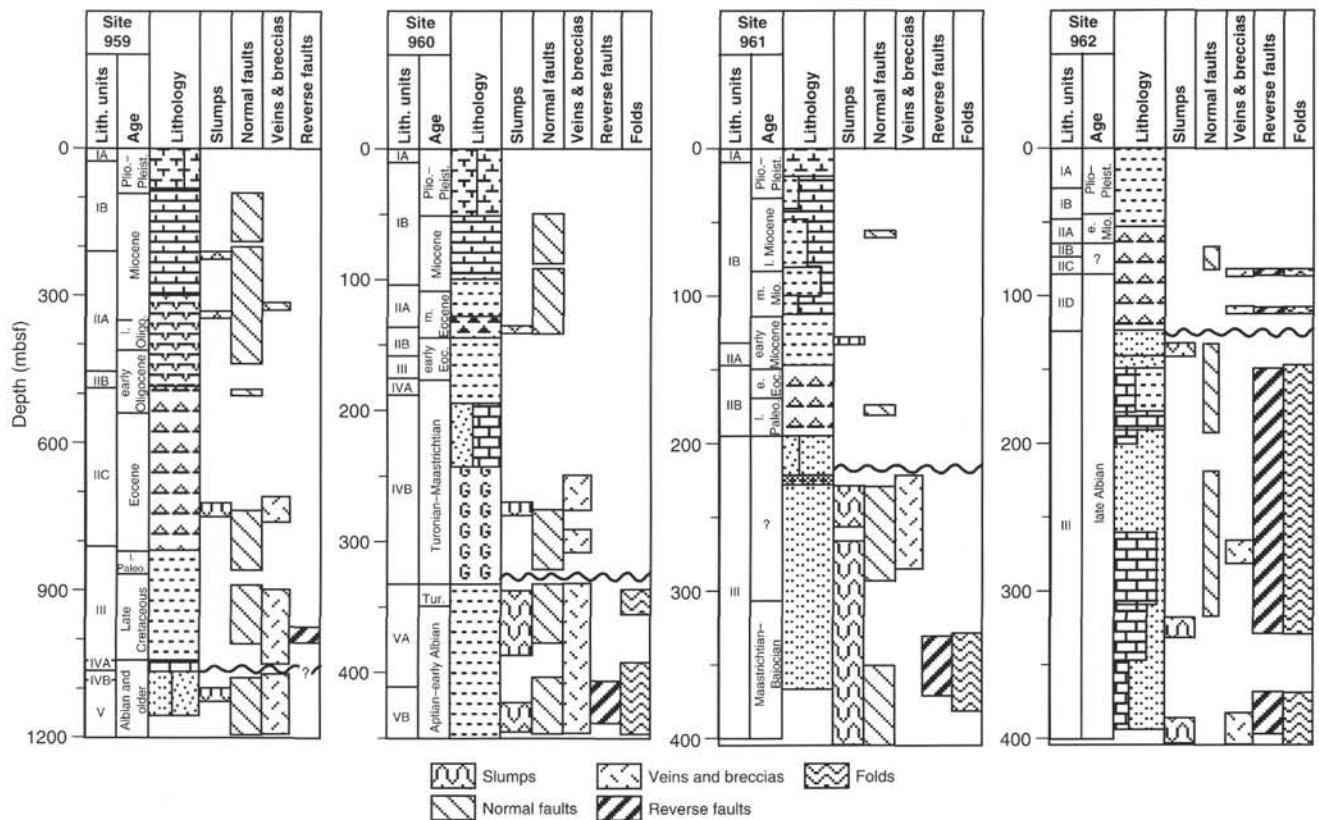


Figure 6. Diagram summarizing the distribution of structures and deformation styles at all four sites. Lithology symbols are given in the "Explanatory Notes" chapter.

tectonized sediments of seismic Unit A and the hemipelagic cover above. At Site 960 the most prominent break is between Eocene claystones (lithologic Subunit IIB and Unit III) and the carbonate-cemented sandstones and limestones dated as Turonian-Santonian in age (lithologic Unit IV). These are considered to be seismic Unit B, and may postdate the active transform tectonism, at least in part. The low porosities measured here are attributed to the pervasive cementation and diagenesis affecting these sediments. At Site 959 there is a broad pattern of decreasing porosity downsection. Again, the lowest porosities are found in Albian strata (lithologic Unit V), and an increase to higher porosities is seen across the transition into the overlying redeposited carbonates (lithologic Unit IV), which are also notably less tectonized.

At Sites 960, 961, and 962 the effects of slumping and tilting due to faulting result in a section showing no systematic variation in structural style from top to bottom. Strong coring-related disturbance may also have observed any pattern in the deformation style. High bedding dips (almost vertical in some cases) were recorded within the Lower Cretaceous sections, especially in lithologic Unit V in Holes 959D and 960A and in lithologic Unit III in Holes 961A and 962D (seismic Unit A). Small-scale asymmetric folds in Hole 962D suggest that the steep dips in that section are related to large-scale folding. All of these features are interpreted to be the product of deformation within a major transform zone.

Structures Related to Soft Sediment Deformation: Syn- or Early Post-depositional Phases

Normal faults of a clear syndepositional origin are relatively rare. However, in the Cretaceous sections (lithologic Unit III) of Hole 961B, variations in thickness were noted in beds on either side of normal faults. Water-escape structures were found in the Lower Cretaceous of Holes 960A and 961A. Convolute lamination is largely re-

stricted to the deepest parts of Holes 959D, 960A, and 962D, where it is closely associated with slumping. Slumping is significant in Miocene sediments at Site 959 (Fig. 6), where it is accompanied by numerous normal faults, larger examples of which are also seen in the multichannel seismic lines.

All of the early deformational structures are probably related to basin instability during deposition of Albian and older lithologic Units III (Sites 961 and 962) and V (Sites 959 and 960). This deformation, related either to slope instability or to seismic shocks, is a direct consequence of active tectonism in a pull-apart setting during the syntransform phase.

Post-depositional (Synlithification to Post-lithification) Structures

Evidence for compressional and extensional stresses is noted at all four sites. Direct evidence for strike-slip deformation is sparse but is seen at Sites 960 and 962.

Normal faulting is ubiquitous in sediments at all stratigraphic levels, occurring at all four sites (Figs. 8A, 9). However, a differentiation can be made according to the nature of the fault planes and their geometry (shape and attitude). Several types were observed. Hole 959D displays two main types: (1) anastomosing fault planes enclosing lenses of sheared material, which are post-dated by (2) planar, normal faults, which clearly reflect more lithified conditions (Fig. 9). Normal faults, which reflect extension, may have occurred as a result of trans-tensional stresses within the overall transform zone.

Reverse faulting is less common and is locally associated with regions of intense normal faulting (e.g., in the black claystones of lithologic Subunit VB, Hole 960A) and is found closely associated with microfolding (Figs. 8B, 9). It occurs in Cretaceous sediments of Albian or older age (Holes 960A, below 330 mbsf, 961B below 330 mbsf, 962D below 123 mbsf), and may be found in sediments as young as the Coniacian in Hole 960C. Shear faulting was rarely ob-

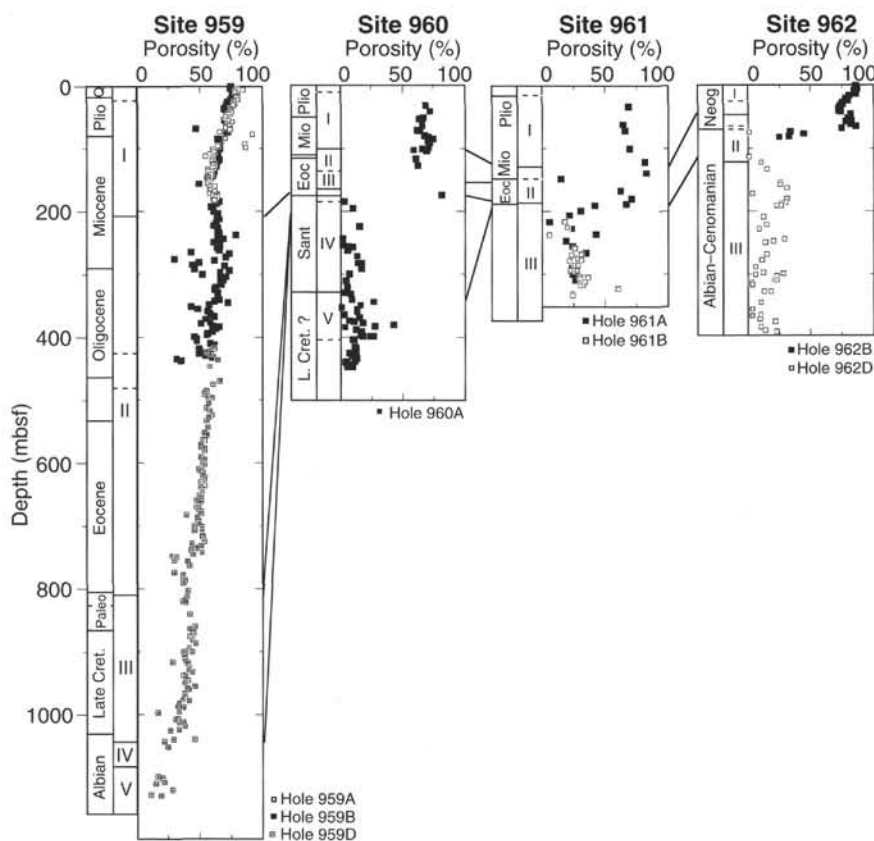


Figure 7. Diagram showing the variation in porosity measurements at all four sites, and especially the strong difference between Cretaceous and Cenozoic rocks. Also note the break at 750 mbsf at Site 959, which also correlates with a break in strong faulting seen below, compared to undeformed above.

served and is found in both shallow- and steep-dipping intervals (e.g., Fig. 8C) of variable width. Shear zones in the Cretaceous at Site 961 show the highest intensity of deformation, with the development of an incipient crenulation cleavage. In Hole 961B, a 20-m-thick zone between 330 and 350 mbsf may be interpreted as one of the major shear zones, running along the Côte d'Ivoire-Ghana Marginal Ridge.

Small-scale folding was observed at Sites 960, 961, and 962 and is relatively common in Hole 962D, where the folds occur exclusively in lithologic Unit III and range from brittle kink folds to soft sediment folds. This suggests that deformation was a continuous process that affected the sediments both during and after lithification. The folds are mainly asymmetric with rounded to angular hinges and are commonly cut by reverse faults along the short limb. Incipient kink folds, with associated reverse faults nucleating along fold axes, are observed. Pop-up structures develop in cases where the faulting has progressed to a more advanced stage. Compressional effects also are recorded by localized development of cleavage. For example, bedding-parallel cleavage is well expressed in the fissile claystones of lithologic Subunit VA in Hole 960A. Microfolding with incipient crenulation cleavage is locally well preserved in lithologic Unit III in Hole 961B.

Evidence for strike-slip motion is rare and was only observed in Holes 960A and 962D. In lithologic Unit V in Hole 960A, kaolinite-filled fractures and veins display mineral lineations that give a clear strike-slip sense of motion. A minor fault structure, displaying both normal and reverse senses of motion, was observed in lithologic Unit III in Hole 962D. This may reflect larger scale flower structures related to strike-slip motion. Oblique slickensides observed deeper in Hole 962D indicate a significant component of strike-slip motion.

Veining occurs at all four sites and is particularly abundant in Holes 960A and 962D. Several different vein minerals were observed, including kaolinite (Hole 960A), calcite (Holes 960A and 962D), pyrite (Hole 959D), quartz (in Core 159-960A-61R), and barite (Holes 959B, 960A). Vein minerals commonly infill fractures and

fault zones (Figs. 8D, 9), open tension gashes, cements in breccia zones, and occur as scattered, irregular patches within the sediments. Calcite veins are the most abundant variety and commonly display more than one generation of vein fill. In Hole 962D they form well-developed conjugate sets that postdate folding and faulting, but appear to predate tilting of bedding.

Thermal Alteration/Diagenesis of Clays and Organic Material

Thermal maturation of the clays in sediment recovered during Leg 159 is indicated by the progressive disappearance of the more labile smectite group clays and the appearance of both chlorite and progressively nonexpandable illite-smectite, mixed-layer clay minerals (Fig. 10). Chlorite is pervasive in seismic Unit A sediments from Sites 960 (lithologic Unit V) and 961 (lithologic Unit III), which, in the absence of mixed-layer clays, indicates this sediment has been affected by high temperatures, unlike the overlying sequences. Moreover, mixed-layer clays are more ordered in the sediments of lithologic Unit III at Site 961 ($R = 3$ vs. $R = 0$; Moore and Reynolds, 1989), indicating either that this sediment reached a higher temperature during burial than that at Site 960, or that it was subjected to a high temperature for a longer period of time. In contrast, chlorite is present in only a trace amount in a few samples from lithologic Unit III at Site 962. The co-occurrence of expandable mixed-layers suggests a detrital origin for the chlorite from the top of lithologic Unit III (seismic Unit A) at Site 962. This chlorite may have been derived from more thermally mature sediments eroded elsewhere in the area. No samples from lithologic Units IV and V at Site 959 were examined by XRD, but of the five black claystone samples analyzed at this site (lithologic Unit III), only a trace amount of chlorite was identified in one sample. In this unit, the dominant clay is of the smectite group and appears to be highly expandable, further supporting evidence that upper Santonian-upper Paleocene sediment from this unit has not been subjected to high-temperature diagenetic conditions.

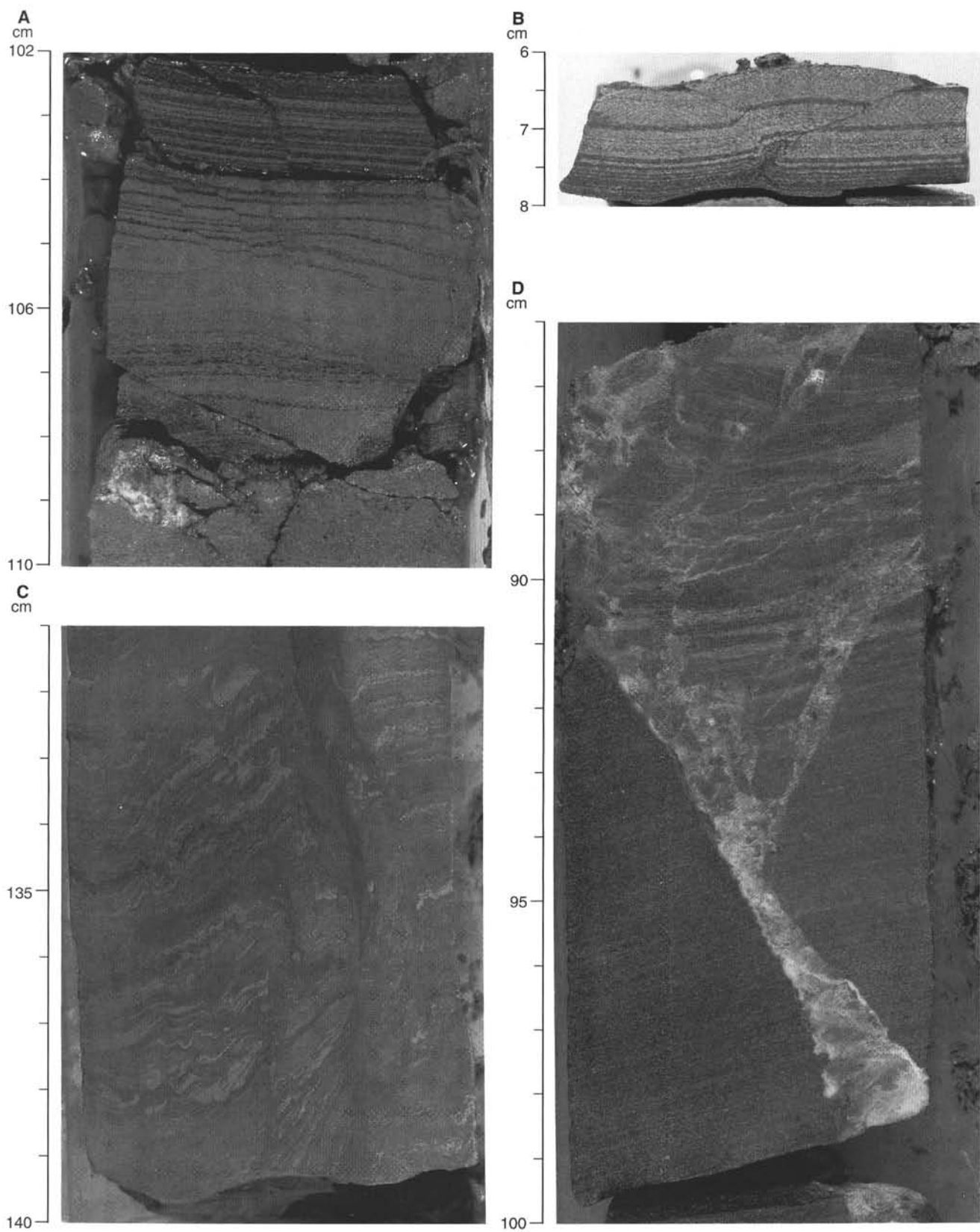


Figure 8. Photographs of the most common structures seen in the core, showing the association of both normal and reverse faulting within the transform zone. **A.** Normal fault (159-959D-73R-1, 102–110 cm). **B.** Microfolding associated with reverse faults resulting in a pop-up structure that is common in Hole 962D (159-962D-27R-CC, 6–8 cm). **C.** Vertical shear faults with tight associated microfolding in laminated siltstones (159-961B-13R-1, 131–140 cm). **D.** Fault with breccia and calcite mineralization (159-960A-46R-1, 86–100 cm).

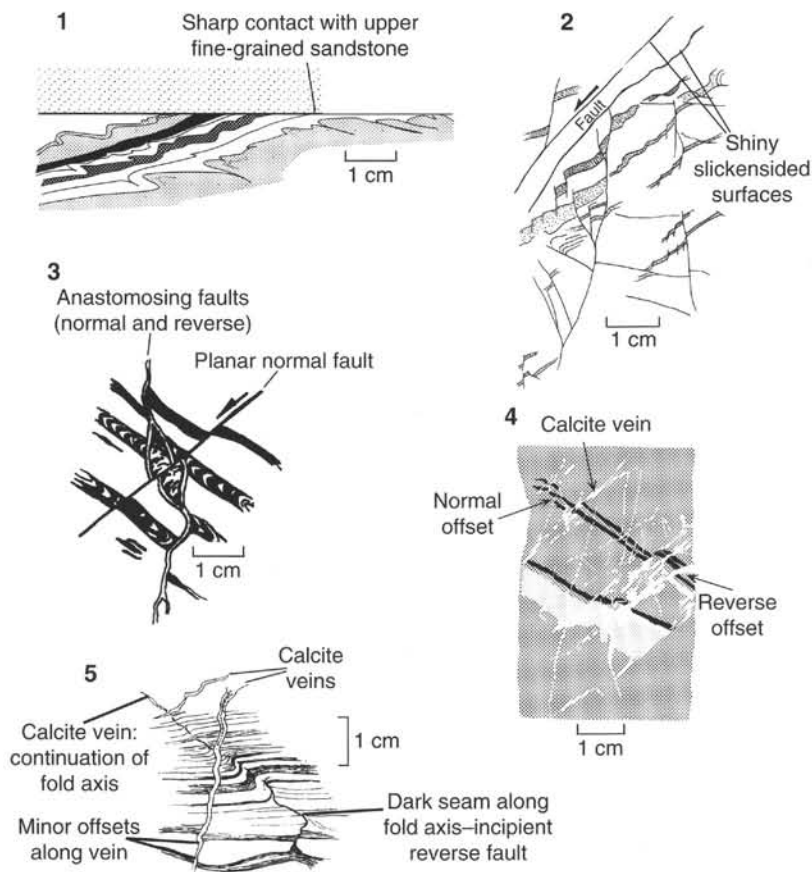


Figure 9. Detailed sketches of microstructures seen in the cores, representative of the variety of deformation styles throughout tectonized seismic Unit A. **1.** Slump showing evidence of shear. The short limbs of asymmetric microdrag folds are sheared and pass into small reverse faults (interval 159-960A-59R-2, 60–62 cm). **2.** Set of conjugate normal faults with associated reverse faults concentrated in footwall of a larger fault zone (interval 159-961B-18R-2, 75–86 cm). **3.** Normal faults in porcellanites and micrite cutting across burrows (interval 159-959D-43R-3, 81–88 cm). **4.** Set of conjugated normal faults formed prior to tilting. Calcite occurs as infilling of the faults (Section 159-962D-6R-CC). **5.** Asymmetric microfold with incipient reverse fault along axis, cut by calcite vein (interval 159-962D-26R-1, 64–71 cm).

The record of thermal alteration of seismic Unit A (i.e., the pre-Turonian) is also supported by Rock-Eval data. At Sites 959–962, T_{\max} values indicate that organic material from these sediments is over-mature. Given the present depths of burial and the geothermal gradient, this degree of organic matter maturation is not likely without additional thermal perturbations related to deeper burial and/or heating, probably during a deformational event.

II. Marginal Ridge Emergence Stage: Coeval Carbonate Reef and Siliciclastic Deposition

Termination of Syntransform Stage—Depositional Character

The end of the syntransform stage is marked by a maximum in the uplift of the Marginal Ridge and subsequent cessation of active transform tectonism. These two effects result from the presumed passage of an oceanic spreading center south of the margin at that time (Basile et al., 1993; Fig. 5). This change is recorded in the stratigraphy at each site as an unconformity. An erosional unconformity at Site 960 is dated as Turonian. At Site 959, an angular unconformity has developed that is dated as Late Albian to Turonian. Timing of the unconformities above the tectonized sediments of seismic Unit A (at Sites 961 and 962) is not well constrained.

The sediments overlying the unconformity at Site 960 and their lateral equivalents at Site 959 are periplatform deposits, debris and grain flows from a shallow shelf setting (rimming reef) into an adjacent basin. Importantly, the thickness of the limestones increases

from 40 m at Site 959 to 140 m at Site 960. This, in addition to a northward transport direction inferred from FMS logging, suggests that these reefs colonized shallow regions associated with the crest of the uplifted Marginal Ridge (Fig. 4). Moreover, examination of the clastic component indicates an overall coarsening of siliciclastic grains southward toward the ridge crest. This may imply that clastic grains had their source from uplifted regions of this ridge, or from continental fragments associated with the South American Margin. Carbonates at Sites 959 and 960 are dated from Turonian through Coniacian and represent the shallowest water sediments seen on the ridge crest. Their deposition is thus inferred to represent the time of maximum uplift, possibly coincident with the passage of the oceanic spreading center south of the margin at that time. We can imagine the reworked carbonate debris being derived from a reef complex close to the crest of the Marginal Ridge: the ridge (and reef?) migrated westward with the point of maximum uplift that shadows the intersection of the oceanic spreading center with the transform margin. If that were the case, then this has implications for the source of the clastic material. A source on the South American Margin is suggested by the presence of abundant feldspar and angular quartz (both igneous and metamorphic origins), which appears less mature than would be anticipated if all the sediments were recycled from uplifted sediments of the underlying Albian sandstones. However, it is difficult to see how the clastic component could have been derived from the South American Margin, if the uplift reflects passage of the spreading center, as this would have ceased to lie adjacent to the Marginal

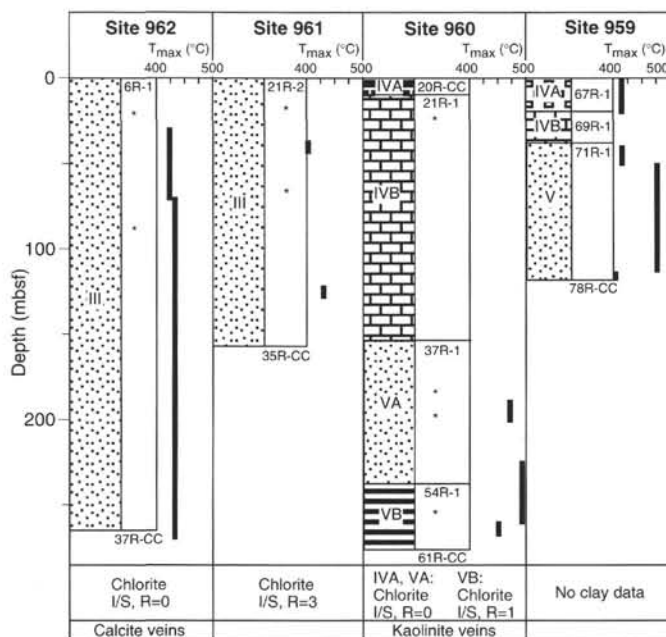


Figure 10. Diagram showing the variation in the degree of thermal maturation of the sediment column at all four sites, through use of the Rock-Eval analysis of organic carbon to determine T_{max} values. Note higher degree of thermal maturation of the Lower Cretaceous and the distinct jump in thermal maturity in the Santonian–Coniacian of Site 959. Datum = top of syntransform tectonized sediments. * = sample location for XRD analysis.

Ridge at the end of the continent/continent transform phase. It is noteworthy that although a record of ridge uplift and tilting is preserved at Sites 959 and 960, almost none of this record is present at Sites 961 and 962, due to the large unconformities generated there.

Termination of Carbonate Deposition

Termination of the carbonate sedimentation implies a dramatic change in the depositional environment. The very high upward accretion rates of reefal complexes typically exceed rates of tectonic subsidence. Thus, upward growth is maintained unless reef growth is inhibited by detrital influx or a rapid change in relative sea level. Importantly, there is no evidence for termination of reef growth by the influx of clastic detritus. Instead, this region appears either to have undergone a phase of rapid subsidence, or a change in oceanographic conditions, such as current activity or salinity changes, which would make high rates of carbonate production unfavorable. Given the coincidence of termination of reef growth with the cessation of siliclastic input from the ridge, a regional deepening of the basin and ridge is a more likely cause for this transition.

III. Passive Margin Stage

Following the demise of shallow-water carbonate sedimentation after the late Santonian, the dominant tectonic setting for sedimentation can be characterized as a passive margin. Overall, the sharp tectonically controlled contrasts in sedimentation, between uplifted or down-faulted basins, gave way to deepening of the basin and progressive submergence of the margin on a regional scale. In general, control of the depositional setting progressively shifted from local tectonic factors to global-scale oceanographic factors (Figs. 4, 5). This is reflected by three subdivisions during the passive margin stage: (A) oceanographic differentiation of the Deep Ivorian Basin; (B) an in-

crease in biosiliceous sedimentation; and (C) pelagic and hemipelagic sedimentation. These phases are recognized on a regional scale, although the principal causes of these transitions are not fully resolved.

Differentiation of Deep Ivorian Basin and Marginal Ridge

Following the demise of shallow-water carbonate sedimentation after the late Santonian, the most significant change to affect the sedimentation in the area was the cessation of coarse-grained clastic input into the Deep Ivorian Basin (Site 959) and to Sites 960–962, which occupy the crest of the Marginal Ridge. In addition, while there was some evidence for the development of a depositional basin to the north of the Marginal Ridge during shallow-water carbonate deposition, oceanographic conditions were similar at both the ridge and basin settings. Redeposited limestone sequences at both Sites 959 and 960 are overlain by pelagic deposits of Late Cretaceous age. This situation changed after the late Santonian, when the conditions at Site 959 showed a marked difference from those at Site 960 (Figs. 4, 5).

At Site 959, lower Coniacian sandy limestones are disconformably overlain by a condensed sequence of dark gray clayey nannofossil claystones spanning the upper Coniacian through upper Santonian. Interbedded within this condensed interval are at least two phosphatic, nodular hardgrounds composed of phosphatized pellets, glauconite grains, fish debris, and phosphatized pelagic carbonate. In addition, this interval contains a graded conglomerate with clasts apparently derived from the erosion of a preexisting phosphatic hardground.

This condensed pelagic carbonate interval is overlain by a 209-m sequence of organic-rich black claystones devoid of biogenic carbonate or silica. Pyrite, barite, and glauconite occur throughout, and commonly preferentially fill the *Chondrites* and *Zoophycos* burrows that disrupt the primary bedding laminations. The age of the sequence is uncertain, although it is bracketed by upper Santonian sediments below and middle upper Paleocene strata above. In addition, preliminary palynological data suggest that at least the lower 155 m is Late Cretaceous in age. Assuming that this interval spans the entire late Santonian through middle late Paleocene yields a minimum sediment accumulation rate of 7.5 m/m.y. for the noncalcareous claystone sequence. Diverse agglutinated benthic foraminiferal assemblages indicate that the sediment-water interface was upper bathyal to abyssal in depth and poorly oxygenated. This assemblage is cosmopolitan within flysch-type settings from the Atlantic during the early Paleogene through the Late Cretaceous (Gradstein and Berggren, 1981).

Organic carbon in these black claystones consists of a mixture of terrestrial and marine organic matter of low to intermediate thermal maturity. Organic carbon contents are elevated, reaching peak values of 5.5 wt%. However, there are significant fluctuations in the wt% organic carbon and the hydrogen indices throughout this sequence. These fluctuations, and the episodic nature of bioturbation through the sequence, indicate that the sediment was subject to dysaerobic conditions of varying intensity during deposition. These variations are consistent with fluctuations in productivity and/or variations in the depth and strength of an oxygen minimum zone impinging on the outer continental slope. This variable, dysaerobic regime may have been enhanced by partial silling of the basin by the Marginal Ridge, although this was not necessary to achieve the observed effect, given the generally stagnant nature of the Late Cretaceous oceans.

Near the crest of the Marginal Ridge, the entire upper Santonian to upper Paleocene section is represented by a highly condensed, 23-cm-thick section of upper Coniacian to Santonian micritic nannofossil claystone capped by a 1-cm-thick phosphatic hardground. The phosphatic hardground itself contains nannofossils of Santonian age as well as rare specimens of Maastrichtian planktonic foraminifers, indicating a prolonged history of exposure at the seafloor. The deposition of such an extremely condensed sequence indicates a deposi-

tional environment that was swept by currents, with only rare respites that allowed sediment accumulation. Appreciable phosphatic mineralization most often occurs only during episodes of advection of nutrient-rich, oxygen-depleted, intermediate waters (Watkins et al., in press).

The lithologic contact between the Albian(?) clastics and the Paleocene pelagic sediments at Site 961 was highly disturbed by drilling, making it difficult to assess the nature of the contact. It is clear, however, that little or no sediment is preserved that records the Late Cretaceous and early Paleocene history at this site. The presence of abundant glauconite in the overlying upper Paleocene porcellanite suggests that the transition may be marked by a glauconitic hardground, as occurs at Site 962.

The upper Albian clastics at Site 962 are overlain by a sequence of black, organic-rich porcellanite with clay containing ammonites and silicified planktonic foraminifers and radiolarians indicating a late Albian to Turonian age. This unit is similar to those reported from the northwest African Margin (DSDP Sites 137, 138, and 415; Wolfart, 1982) and appears to record the earliest fully oceanic deposit recovered during Leg 159. Much of the chert and porcellanite in this unit has been fractured and annealed with clear chert, indicating that the porcellanite brittlely fractured subsequent to its transformation from opal-A to opal-CT. The timing of this event is uncertain, although it is known that the transformation can occur within a geologically short period of time. Interpretation of the stratigraphic placement is obfuscated by the poor core recovery (with an incomplete APC stroke and flow-in), although it appears to be overlain by a complex hardground or hardgrounds characterized by both manganese oxyhydroxide crusts and glauconitic hardgrounds and lag deposits.

These relatively thin stratigraphic records at the Leg 159 sites indicate that much of the area was undergoing sediment starvation through the Late Cretaceous. The basin, represented by Site 959, was receiving minimal fine-grained clastic influx from the African margin. This sediment, deposited in upper bathyal depths, ponded behind the Marginal Ridge and was subject to episodic dysaerobic conditions. Similarly, the phosphatic hardgrounds that accreted on the upper bathyal crest of the Marginal Ridge indicate deposition under low oxygen conditions. The presence of manganese oxyhydroxide and glauconite in the hardgrounds at Sites 961 and 962 (deposited in lower bathyal and abyssal depths) indicates deposition in relatively oxygenated bottom water conditions. Low-oxygen, upper bathyal waters overlying relatively well oxygenated, lower bathyal and abyssal waters suggest that the dysaerobia in the Deep Ivorian Basin was the result of an expanded oxygen minimum zone.

Beginning in the late Paleocene, calcareous pelagic sedimentation was renewed in the area. This interval of pelagic sedimentation commenced in the late Paleocene (approximately 58 Ma) with chalk deposition that persisted into the earliest Eocene. Sediment accumulation rates for this 4–5 m.y. interval of chalk deposition were quite low (<7 m/m.y.), suggesting sporadic sedimentation and preservation. However, the change from starved basin conditions to pelagic calcareous sedimentation signals the integration of the area into the larger Atlantic system. This upper Paleocene chalk is also the youngest stratigraphic unit that shows evidence of significant, pervasive extensional stress as indicated by faulting and fracture fill structures (Fig. 6). The top of this chalk also corresponds with a significant shift in porosity and acoustic velocity (Fig. 7).

Biosiliceous Sedimentation

Beginning in the early Eocene, and continuing into the early Miocene, oceanographic conditions that generated biosiliceous sediment throughout the world oceans influenced sediment deposition at all sites. These sediments comprise of thick sequences of porcellanite, chert, and diatomite. Unique to certain areas, however, was the formation of palygorskite clay during the Paleogene. Claystones en-

riched in, or even dominated by, palygorskite were recovered at Sites 960, 961, and 962. They occur in lower Eocene calcareous nannofossil Zone CP10 at Sites 960 and 961, and may be the same age at Site 962 based on facies similarities. This zone represents an unusual depositional setting whose environmental significance is poorly understood. Based on current models of the formation of palygorskite clays, resolution of the origin of these claystones could constrain the depositional environment of this region, and, in particular, of the Marginal Ridge during the early Eocene.

Although it is undisputed that palygorskite forms in arid soils and lagoonal environments, the origin of palygorskite in oceanic basins remains strongly debated. This debate, reviewed by Singer (1979), Kastner (1981), Jones and Galán, (1988), Chamley (1989), and Weaver (1989), has two general lines of reasoning, which will be called the "authigenic model" and the "detrital model."

The "authigenic model" assumes that palygorskite principally, or even exclusively, forms at the ocean floor, either by direct precipitation or by transformation of a precursor mineral. The strength of this model lies in its ability to explain the occurrence of palygorskite in areas where detrital input plays a minor role, as at mid-oceanic ridges and abyssal plains. A major difficulty of the model, however, is the disagreement concerning whether palygorskite can actually form at sea-bottom conditions. Palygorskite cannot be precipitated from normal seawater (Kastner, 1981); however, higher temperatures (above 25°C) would allow palygorskite to precipitate. For example, the alteration of submarine basalt has been reported as a source for both the required magnesium and heat.

The "detrital model" proposes that most or all of the palygorskite found in deep-sea sediments has been reworked from either shallow-marine or terrestrial environments where it formed authigenically. The "detrital model" has been invoked in particular for the middle Cretaceous and Paleogene palygorskite occurrences in the eastern Atlantic Ocean (Chamley and Debrabant, 1984). Several coeval palygorskite deposits could be identified on the adjacent shelves or terrestrial areas, which could be the source for deep-sea deposits. Supply mechanisms would include fluvial erosion, sediment-gravity currents, and erosion and transport by wind. The major shortcoming of the "detrital model" is the discontinuous occurrence of palygorskite on many transects from the proposed source to the final site of deposition. Thiry and Jacquin (1993) pointed out that there is a remarkable gap in reported palygorskite occurrences in the shelf and slope environments and concluded that shallow- and deep-water palygorskite deposits are genetically unrelated.

Palygorskite claystones from Leg 159 are neither clearly detrital nor authigenic. The comparatively pure occurrences of this mineral are suggestive of an authigenic origin. Although minor amounts of other clay minerals and silts are intermixed, these may reflect eolian transport and subsequent intermixture at the site of palygorskite formation. In the absence of a volcanic precursor, or other lithologies that could be altered to palygorskite, an authigenic origin would require conditions of elevated temperatures with increased salinities and alkaline conditions. Such an environment could develop if shallowing of the Marginal Ridge by uplift or sea-level fall (Fig. 4) produced locally restricted and hypersaline conditions. Such a scenario is problematic, however, when the ecology of associated foraminifers is considered.

Benthic foraminiferal assemblages at Site 961 indicate lower bathyal to abyssal depths from at least the Eocene to the present. This is of particular importance given that the palygorskite zone lies within this lower Eocene to upper Paleocene interval. Specifically, at Sites 961 and 960, palygorskite claystones are over- and underlain by sediments containing a benthic foraminiferal assemblage of *Bulimina*, *Cibicidoides*, *Pyrimida*, *Nonion*, and *Nuttallides* that suggests bathyal to abyssal depths of deposition. Lower Eocene palygorskite clays at Site 961 also contain abundant specimens of *Quadratobulimina pyramidalis*, *Aragonia velascoensis*, and *Gyroidinoides*

globosa—all species indicative of intermediate to deep water conditions. The presence of radiolarians in these clays at both sites is also inconsistent with a nearshore site of deposition. Despite the enigmatic origin of this clay mineral, resolution of its diagenetic or depositional origin could refine our understanding of the environmental conditions present in this region during the early to middle Paleogene.

Following deposition of palygorskite claystones was a period of high biosiliceous productivity that persisted in this area from the late early Eocene to early Miocene. The most complete section of biosiliceous sediment was recovered at Site 959, and comprises 604 m of porcellanite, chert, and diatomite interbedded with pelagic calcareous sediment. Clay is a variable and usually minor component. The upper 219 m at Site 959 is least affected by diagenesis, with excellent preservation of diatoms, silicoflagellates, and less abundant radiolarians. At Site 960, the principal siliceous component is radiolarian, suggesting increased winnowing at that site. This is consistent with its more topographically exposed location. Lower Oligocene to upper Paleocene sediment at all sites is mildly to heavily affected by dissolution of both siliceous and calcareous components. The opal-A of biosiliceous tests has been recrystallized to opal-CT (identified by XRD), generating porcellanite, and calcitic nannofossils and foraminifers have been partially altered to micrite. Chert formed below and above porcellanite, and ranges in age from early Eocene to early Oligocene. Despite local diagenetic overprints, primary sedimentary features such as bedding and component variation are consistent throughout biosiliceous deposition.

The principal components of sediment in this interval—diatoms, nannofossils, clay, and minor silicoflagellates, radiolarians, sponge spicules, and foraminifers—alternate, generating beds 10 to 80 cm thick. Biosiliceous-rich beds are dark brown, reflecting higher contents of organic matter and pyrite. Increased levels of clay or nannofossils form lighter colored beds. Contacts between interbeds are generally gradational due to moderate bioturbation. Abundant trace fossils include *Zoophycos*, *Chondrites* (more evident in the darkest beds), and *Planolites*. The only disruption to this pattern is a 25-cm-thick, crudely graded bed of intraclasts (i.e., granules and pebbles of diatomite and chalk), interpreted as a debris flow that was recovered at Site 959. This bed is age-correlative to chaotic, slumped beds at Site 960.

Age control within this biosiliceous interval, based on both calcareous and siliceous microfossils, indicates that sediment accumulation rates averaged approximately 15–22 m/m.y. throughout the Eocene to early Miocene. However, rates for the late Eocene and much of the Oligocene have been extrapolated from stratigraphically adjacent control points. Organic carbon contents of these sediments are high and are dominated by marine organic matter. No phosphate was detected during sedimentological analysis. The high levels of marine organic content, lack of sedimentary phosphate, and relatively moderate sediment accumulation rates indicate that this area experienced sustained levels of productivity throughout the late Paleogene and earliest Neogene.

Pelagic and Hemipelagic Sedimentation

The Neogene succession in the Côte d'Ivoire Basin comprises a thick sequence of pelagic and hemipelagic oozes and chalks containing abundant nannofossils and foraminifers. The thickest and most complete Neogene section was recovered at Site 959 in Holes A, B, and C. Similar sediment, but a thinner section, was recovered at Sites 960 and 961. All three sites were well above CCD throughout the Neogene (see the "Biostratigraphy" sections of site chapters, this volume). Two end-member sediment types, nannofossil ooze, and foraminifer ooze (changing to chalks at depth), occur in varying proportions, forming 10- to 80-cm-thick interbeds of nannofossil foraminifer ooze, nannofossil ooze, foraminifer nannofossil ooze, etc. Increases in nannofossil content may be related to coccolith produc-

tivity; and increases in foraminifer content are probably related to enhanced winnowing of bottom sediment.

Clay becomes an important third component in the Miocene part of the section, and variations in the clay content are best reflected in the carbonate abundance data. The decrease in clay content upsection may be a dilution effect caused by deposition or preservation of enhanced carbonate. Alternatively, there could have been a decrease in delivery of terrigenous clastics to this site during the Miocene to Holocene. The clay may be eolian or reworked from more nearshore, fluviially derived sediment. The principal detrital mineral components (from XRD) include a mixed-layer illite/smectite mineral, kaolinite, discrete illite, and quartz, the latter two being more abundant in the silt fraction. Traces of plagioclase, K-feldspar, and gibbsite ($\text{Al}(\text{OH})_3$) occur locally and are observed in bulk samples and clay separates.

The input of these prime components (nannofossils, foraminifers, and clay) has varied through the Neogene. At times deposition of any of the components has slowed sufficiently for glauconitic hardgrounds to develop. The youngest hardgrounds occur in lower Pliocene sediment (nannofossil Zones and Subzones CN11a, Hole 959A; CN9b, Hole 959B; CN11, Hole 959C). Although glauconite has not been separated from the surrounding sediment, XRD results of clays extracted from hardgrounds suggest that they are formed of mixed-layer smectite. Odin and Matter (1981) suggest that such glauconitic hardgrounds can take 1,000 to 10,000 yr to form.

Other variations observed in the sediment were imposed by changes in bottom current activity and the oxygenation of the bottom waters. Numerous scours are locally overlain by millimeter-thick lags of foraminifer tests and/or glauconite pellets. Variation in the oxygenation of the bottom waters is indicated by alternating intervals of faintly laminated and moderately to heavily bioturbated sediment.

The Neogene sediment has undergone pervasive yet minor diagenesis, much of it involving iron. Throughout the Neogene section, iron minerals fill burrows as siderite or ankerite, glauconite, and/or pyrite. Glauconitization has occurred relatively early, as indicated by glauconite-filled foraminifers in Sample 159-959B-1H-3, 145–150 cm. It is not clear whether pyrite or glauconite formed first, as the material picked from foraminifers in Sample 159-959B-1H-3 contained both. The clay mineral composing the green fill is a mixed-layer illite/smectite. This mineral generally replaces a preexisting mineral, usually kaolinite. Such a process normally takes on the order of 1,000 to 10,000 yr (Odin and Matter, 1981). Glauconite forms color bands, which we interpret as nascent hardgrounds, millimeter-scale pellet lags (laminae), and thin, wispy hardgrounds. Nothing is known yet of how this mineral varies downhole (i.e., with time, climate, sedimentation rates, etc.), but in general, glauconite forms where there is a balance between detrital input and winnowing by marine currents (Odin and Matter, 1981). This occurs where depositional rates are sufficient to preserve organic matter, which provides the sites for iron reduction and mobilization, while bottom currents keep the pellets in repeated contact with a source of Al, Mg, K, and Si. Glauconite development is generally not dependent on climatic conditions, water depth, sedimentation rates, or mineral composition of the sediment (Odin and Matter, 1981).

Carbonate rhombs are also a pervasive, authigenic component of the Neogene sediment. They occur in burrows or as isolated rhombs (first observed in smear slides in Cores 159-959A-11H and 159-960C-8H). Although originally identified in smear slides as dolomite, XRD indicates a mineral composition between siderite and either rhodochrosite (MnCO_3) or dolomite. This indicates variable substitution of Ca and Mg by either Fe or Mn. This is supported by interstitial water chemistry that indicates a diagenetic sink for Mg and Mn (see "Inorganic Chemistry and Diagenetic Reactions" section below).

In addition to a source of Fe for the pyrite, glauconite, and sideritic carbonate from detrital minerals, detrital goethite, $\text{FeO}(\text{OH})$, is observed in Cores 159-960C-10H, and 962A-4H and 5H. Slower sed-

imentation rates and depressed organic matter preservation may account for this rare (at least in the Neogene sediments considered on Leg 159) detrital iron preservation. Goethitic sediment at Site 962 occurs in a pelagic clay sequence (lithologic Subunit IB), deposited at slow sedimentation rates (7 m/m.y.); however, this suggests that glauconitization, including hardground development, may not always occur at the lowest sedimentation rates. Further study is required to isolate and quantify the different processes responsible for these sediments.

Deformational Records

At Site 959, bedding planes dip predominantly toward the north-west–north-northwest and dips increase with depth. This is interpreted as the result of steady subsidence of the Deep Ivorian Basin between the Albian and the early Miocene, in response to progressive cooling of the rifted continental lithosphere (McKenzie, 1978). In addition to direct core measurements, in situ structural measurements were obtained using the FMS tool between 550 and 930 mbsf in Hole 959D and between 190 and 350 mbsf in Hole 960C (Fig. 11). The logged intervals cover the Eocene to lower Oligocene porcellanites (lithologic Subunit IIC) and the upper part of the Upper Cretaceous to lower Paleocene black claystones (lithologic Unit III) in Hole 959D, and the Turonian–upper Santonian limestone unit (lithologic Subunit IVB) in Hole 960C. In Hole 959D, the bedding dips northwest, increasing from 5° to 14° with depth, as expected from the seismic lines (see Basile et al., this volume). In Hole 960C, beds dip to the northeast and show no increase in dip angle with depth. At both sites, dips and azimuths of the bedding exhibit important variations around average values at decimeter to meter scales. These variations are interpreted as cross-bedded or slumped deposits. Associated rotation axes for the slumps were calculated from successive bedding measurements, which mainly trend west-northwest to north-northeast (N300° to N30°) at both sites. The scattering of rotation axes at Site 959 may reflect variations in the strike of the slope with time, or the interfering influences of uplift of the Marginal Ridge and subsidence of the Deep Ivorian Basin.

Interestingly, at Site 959 (Fig. 7), porosity abruptly decreases at about 750 mbsf within porcellanites of lithologic Unit II. Above this level, the frequency of normal faulting and veining also decreases. The Eocene age of this zone does not mark a major tectonic event; however, it does correlate with unconformity surfaces at Sites 960–962, and may represent the end of rapid thermal subsidence and collapse following passage of the oceanic spreading center along the margin (Fig. 5).

NEOGENE PALEOCEANOGRAPHY

Although the selection of sites for Leg 159 was based primarily on tectonic considerations, their geographic and bathymetric locations offer several possibilities for pursuing significant paleoceanographic objectives. The specific paleoceanographic objectives include:

1. Documentation of the character and origin of Atlantic intermediate waters, and a comparison to changes in the strength of the Benguela Current. This will be based on the chemistry of late Neogene benthic foraminifers and the relative abundances of tropical vs. subtropical planktonic foraminifer assemblages taken from the shallowest sites (959 and 960 at about 2 km water depth).
2. Assessment of the relative influence of deep-water flux and local organic productivity on the character of bottom waters in the eastern Atlantic basins. This will be based on comparisons of carbonate and organic carbon preservation between the

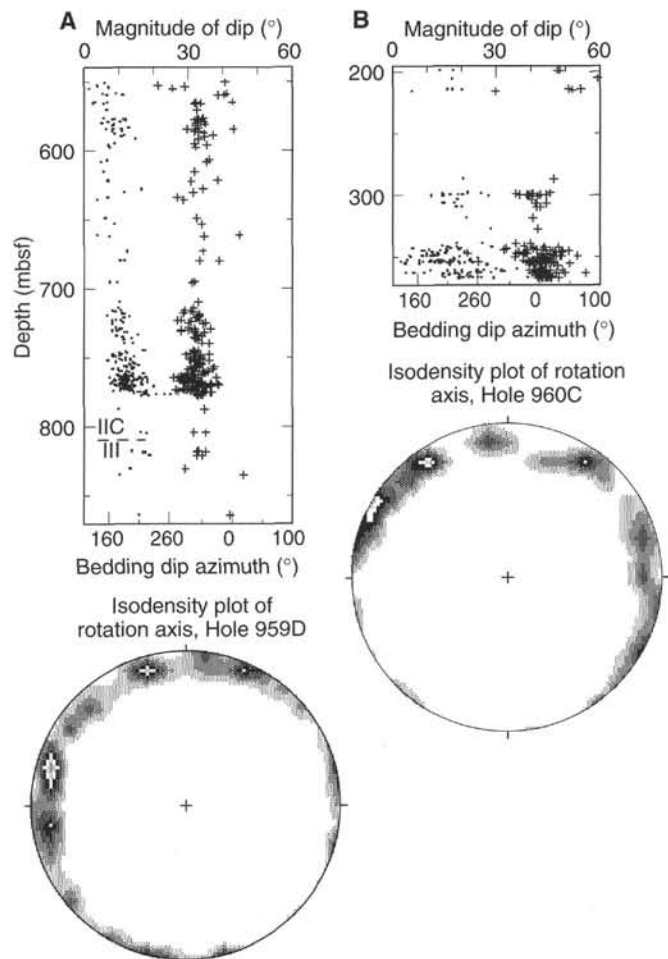


Figure 11. True dips (circles) and azimuths (crosses) of the sedimentary bedding logged by FMS in (A) Hole 959D, and (B) Hole 960C. Horizontal and vertical scales are the same for the two plots. Below each plot a stereographic net (Schmidt net, lower hemisphere) displays isodensity lines (2, 4, 6, 8, and 10%) for 39 rotation axes calculated from bedding dip measurements. For Hole 959D the maxima trend at 260°–300°, 345°, and 030°. For Hole 960C the maxima trend toward 300°–310°, 300°, and 040°.

shallower water sites (959–960) and the deepest site (962 at 4.6 km). Even at the shallowest site, far above the present calcite saturation depth, there is significant calcite dissolution, presumably driven by organic carbon oxidation. At Site 962, in close proximity to the modern calcite compensation depth, sediment carbonate content remained generally low, except during the late Pliocene.

3. Refinement of tropical Atlantic biostratigraphy, which will be based on the composite Neogene section constructed from Sites 959 and 960. The overlap of the siliceous and calcareous intervals during the Miocene will allow precise intercorrelation of calcareous nannoplankton and silicoflagellate biostratigraphies. Realizing the full biostratigraphic potential of these sections will depend on the success of shore-based paleomagnetic studies.

Because they depend on future shore-based analysis, it is too early to know the extent to which the original paleoceanographic objectives of Leg 159 will be achieved. Nonetheless, results from shipboard studies provide some idea of what might be achieved. In particular, they document the age and character of the sedimentary

record and the manner and extent to which it has been modified by diagenetic processes.

Organic Geochemistry

Glacial/interglacial climatic and oceanographic changes are clearly recorded in Pliocene through Pleistocene organic carbon and carbonate carbon profiles at Sites 959–962 (Fig. 12). The highest concentrations, showing large-amplitude and short-term fluctuations, occur at shallower Sites 959 and 960. Farther basinward at Sites 961 and 962, the variability and the relative contents of organic and carbonate carbon decrease, except for the high organic carbon contents in Pleistocene sediments at Site 962.

Carbonate carbon profiles in Leg 159 sediments show intermediate concentrations (40–60 wt%) compared to pelagic sediments, documenting persistent terrigenous dilution throughout the Pliocene and Pleistocene (Fig. 12). An inverse correlation between organic and inorganic carbon reflects the causal relationship between remineralization of reactive organic carbon and the dissolution of calcite.

Shipboard results from Rock-Eval analysis and C/N ratios indicate a strong terrestrial overprint on the marine organic matter signal. Increased supply of terrestrial inorganic and organic material during glacial periods has been reported off northwest Africa (Tiedemann et al., 1989; Sarnthein et al., 1988) and in the eastern equatorial Atlantic, ODP Sites 662, 663, and 664 (Ruddiman and Janecek, 1989; deMenocal et al., 1993). In all these studies eolian transport is interpreted to control the deposition of allochthonous detritus into pelagic areas of the Atlantic equatorial divergence zone. With the close proximity of the African continent, a similar control on organic carbon deposition is assumed for all sites. However, fluctuations in paleoproductivity controlled by Pleistocene glacial/interglacial cycles are evidenced in deposits in the equatorial Atlantic (Verardo and McIntyre, 1994) and off northwest Africa (Stein et al., 1989). However, considering the relatively low time resolution achieved on board Leg 159, variations in organic carbon caused by changes in paleoproductivity cannot be excluded.

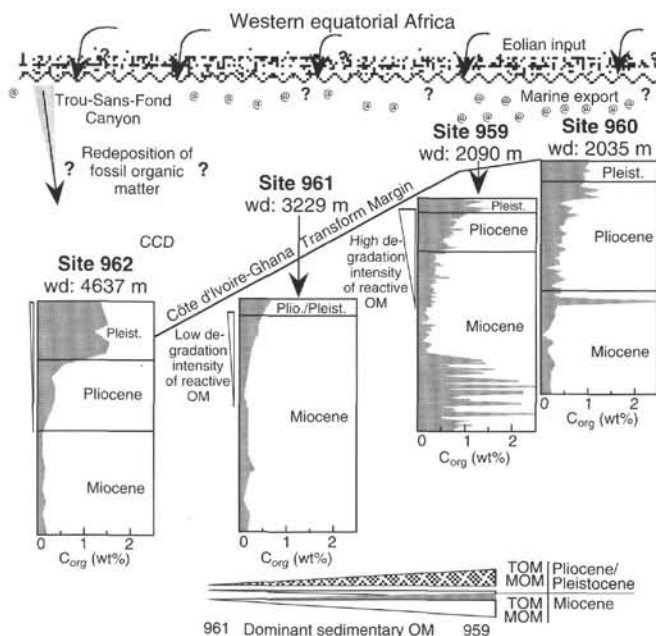


Figure 12. Diagram showing the variation in organic carbon in the sediments at each of the Leg 159 sites for the Neogene, and the contributions of terrestrial (TOM) and marine (MOM) organic matter. Note anomalously high input at Site 962 given its great water depth, attributable to reworked thermally mature Cretaceous organic matter (OM) eroded from the Côte d'Ivoire margin.

The organic matter characteristics of Pleistocene deposits from Site 962 are distinctly different from those obtained at shallower Sites 959–961. Rock-Eval data indicate a dominance of thermally overmature, lipid-rich organic matter as reworked, fossil, organic-rich material. Source areas of this material are presumably submarine Cretaceous outcrops along the transform margin and/or organic carbon-rich sediments transported along the African shelf that were channeled through the Trou-Sans-Fond Canyon offshore from Abidjan. As anticipated from the great water depth of 4637 m at Site 962, which is at about the level of the modern calcite compensation depth (CCD), significant proportions of autochthonous organic matter and of carbonate carbon were not encountered. Quantitative remineralization of labile organic matter within the water column and at the sediment/water interface (Emerson and Hedges, 1988), and intense carbonate dissolution below the CCD, have probably erased most of the original marine signal. However, a temporary deepening of the CCD below the water depth of Site 962 is suggested during late Pliocene times by a sudden rise in carbonate content from about zero up to 20 wt%.

Evidence for long-term diagenetic degradation of reactive organic matter is most obvious in the upper sediment sections at Sites 959 and 960. The general trend, showing a gradual decrease in organic carbon concentration with depth, is interpreted to represent selective mineralization of marine organic carbon (Fig. 12). Compared to the uppermost sample analyzed at Site 959 (0.8 mbsf; 1.0 wt% C_{org}), it can be seen that about 60% of the organic carbon deposited at the seafloor is removed within the upper 90 mbsf (0.4 wt% C_{org}) by diagenetic processes. By comparison, for a similar depth interval at Site 961, the relative diagenetic reduction of organic carbon is even higher (75%), although absolute concentrations in organic carbon are lower and less variable compared to Site 959 (0.63 wt% C_{org} at 1 mbsf and 0.15 wt% C_{org} at 72 mbsf).

Miocene sections at deeper water Sites 961 and 962 show little variation in organic carbon content (Fig. 12). Persistent baseline contents below 0.2 wt% correlate with very low concentrations in carbonate carbon (0 to 10 wt%). A strong contrast between these carbon records and the one derived from Site 959 is most conspicuous for the early Miocene. At Site 959 interbeds of diatomites with nanofossil chinks are clearly recorded by large amplitude, short-term fluctuations in organic carbon and carbonate carbon (Fig. 12). The pyrolytic character of organic carbon-rich diatomites suggests a dominant marine origin for the organic matter, which implies a highly productive depositional environment above Site 959 throughout the late Eocene to the early Miocene. With only a few nautical miles between the sites, it is questionable why the characteristic and extended carbon pattern observed at Site 959 is not recorded in sediments at adjacent Sites 960 and 961. The lack of recovery of time-equivalent deposits may explain the pattern at Site 961. However, at Site 960, lower Miocene sediments were cored and analyzed but still lack an organic carbon and carbonate carbon record comparable to Site 959. The topography of the Transform Margin and the position of Site 960 close to the southern steep slope of the margin may be responsible for the lower organic matter content in lower Miocene sediments. Intense winnowing by focused bottom-water currents at the top of the ridge may have affected the in situ deposition and preservation of organic and carbonate carbon at Site 960.

Inorganic Chemistry and Diagenetic Reactions

Understanding the chemical evolution of interstitial waters is essential for assessing the integrity of the strictly paleoenvironmental record. Depth variations in sediment chemistry reflect the combined influence of depositional changes through time and the integrated effects of water-rock diagenetic reactions. Interstitial water data collected during Leg 159 contribute to our efforts to discern between these two distinct influences on sediment chemistry.

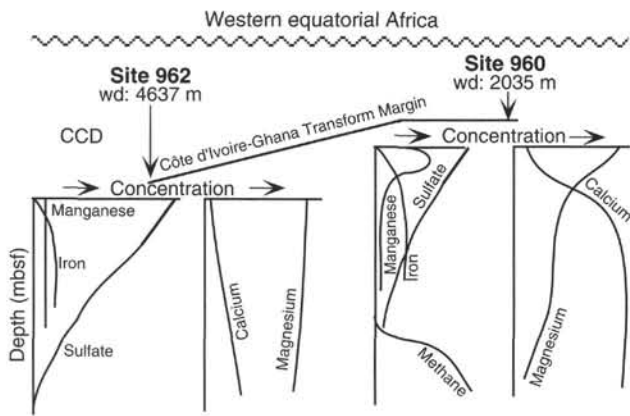


Figure 13. Downhole variation in the concentration of manganese, iron, sulfate, calcium, and magnesium in the pore waters from Sites 960 and 962. The differences are mostly attributable to the relative lack of organic matter degradation in the upper part of the section at Site 962.

One of the goals of further investigations of Leg 159 sediments will be to extract paleoceanographic records documenting changes in ocean chemistry and circulation during the Neogene. As sedimentary diagenesis potentially can compromise the integrity of these records, careful assessment and interpretation of the influence of sediment diagenesis constitute necessary first steps toward meaningful reconstructions of the eastern equatorial Atlantic during the Neogene. It is in this context that we review and summarize the results of interstitial water analyses performed during Leg 159.

In situ diagenetic reactions, fueled by microbially mediated organic matter degradation, exert the primary controls on the chemical evolution of interstitial waters from Sites 959 to 962. At all four sites, a similar sequence of diagenetic reactions is apparent, documenting the gradual transition from oxic conditions near the sediment/water interface to strongly reducing conditions at depth. However, the interstitial water gradients at Site 962 are less steep than at the shallower sites, reflecting the paucity of reactive organic matter and the position of the site below the CCD. Although the complete suite of organic matter oxidants was not analyzed, results of dissolved manganese, iron, sulfate, and headspace methane analyses are sufficient to document the depth evolution of redox conditions within the sediments from each site. A schematic representation of the hierarchy of redox reactions is shown in Figure 13. The complete consumption of dissolved oxygen is inferred from high dissolved manganese concentrations only a few meters below the surface. Only a short distance farther downhole, the dissolution of iron oxides produces elevated dissolved iron concentrations. As discussed below, the depth evolution of the dissolved Fe and Mn profiles appears to be intimately related to the formation of authigenic minerals. Linearly decreasing sulfate concentrations within the pore waters attest to ongoing sulfate reduction within the sediment, with diffusional resupply of sulfate from overlying seawater. Finally, the onset of bacterial methanogenesis is essentially coincident with the quantitative consumption of pore-water sulfate.

The specific depths at which different reactions within the sediment column occur vary slightly from site to site. In general, the vigor of organic matter degradation, as indicated by the downhole increase in ammonium concentrations, decreases with increasing water depth, reflecting the less labile character of organic carbon reaching the sediment/water interface. As a result, the demand for organic matter oxidants decreases with increasing water column length, shifting the depth of the various redox reactions occurring within the sediment deeper below the seafloor.

Organic matter degradation exerts a strong influence on pore-water pH and alkalinity, which, in turn, govern carbonate diagenesis within the sediment. As stable isotope records generated by analyses of benthic and planktonic foraminifers are the main tools for reconstructing paleoceanographic conditions, the nature and quality of carbonate preservation bears heavily on any shore-based paleoceanographic studies. The most significant change in the post-depositional diagenesis of carbonate sediments occurs at the ooze to chalk transition in the upper 80 mbsf in lower Pliocene sediments at Site 959. This zone is a site of carbonate dissolution and redeposition, and these reactions are reflected in the alkalinity and dissolved calcium concentrations of pore waters. Thus, it is possible that results of isotopic paleoceanographic studies based on early Pliocene and older foraminifers could be compromised by diagenetic alteration. There is a marked decline in dissolved manganese concentrations to background levels, coinciding with this diagenetic front, from the maximum observed a few meters below the seafloor (Fig. 13). A sink for dissolved manganese may be its incorporation into carbonate cements, in addition to the formation of rhodochrosite, documented by XRD. Within the biosiliceous lithologies of the Paleogene, calcium concentrations remain high due to dissolution of the few calcareous microfossils in these sediments. Dissolved strontium concentrations also increase with depth, reflecting calcite dissolution and/or recrystallization. In contrast, the decrease in magnesium concentrations with depth appears to be primarily controlled by silica diagenesis within the Miocene diatomites and Paleogene chert and porcellanites.

Diverse authigenic iron minerals were recovered, including pyrite, glauconite, and siderite. These minerals are important in that they are often interpreted as indicators of specific sedimentary environments. For example, glauconite is commonly considered to represent a mildly reducing, current-swept depositional environment. The dissolved iron profiles from Sites 959, 960, and 962 are varied, suggesting subtle differences in iron chemistry between the sites. In all instances, the pore-water data, in conjunction with smear-slide analyses, suggest ongoing mobilization of iron from detrital sources. Most likely, authigenic iron minerals representing more reducing conditions are forming at the expense of iron-containing minerals such as glauconite. Thus, because authigenic iron mineral formation continues throughout much of the sediment pile on the Côte d'Ivoire-Ghana Transform Margin, inferences regarding depositional conditions based on authigenic iron minerals must be made cautiously.

Neogene Biostratigraphy and Paleoceanography

Surface water temperatures and the structure of the upper water column in the eastern Atlantic are very sensitive to small changes in climate and circulation. The eastern basins of the Atlantic are less stably stratified than the western "warm pool" Atlantic and are consequently very sensitive to changes in wind speeds and the strength of the cool-water Benguela and Canary currents. Therefore, analysis of faunal assemblages and isotopic records from Leg 159 sites should provide a detailed record of eastern equatorial Atlantic paleoceanography and climate of Sahelian Africa. However, some of the broader aspects of Neogene paleoceanography can be addressed, given the preliminary data available.

The Neogene stratigraphic record from Leg 159 includes three APC sites located at different depths and topographic settings that will allow the discrimination of effects caused by surface water productivity changes, changes in relative intermediate water current velocities, and variations in the corrosiveness of deeper water masses. The continuous record of pelagic sedimentation at shallow Site 959 indicates a complex history of variations in surface water productivity throughout the Neogene. The somewhat discontinuous record at Site 960 reflects pelagic sediment accumulation at a topographically exposed location within the intermediate water mass. Site 962

records pelagic sedimentation at a topographically exposed location within the deep (>4500 m) part of the water column.

Oligocene to Early Miocene Biosiliceous Event

Relatively high rates of biogenic siliceous and, to a lesser extent, calcareous planktonic productivity characterized the early Miocene, as is evident from the elevated sediment accumulation rates for this part of the section (Fig. 14). This same interval was characterized by large-scale slumping at topographically exposed Site 960, where the regionally higher rates of sediment accumulation may have resulted in local slope instability and failure. Similar slumps of early Miocene age occur on the western margin of the North Atlantic, where they are known as the Great Abaco Member (Jansa et al., 1979).

Of special interest are the cyclical variations in siliceous and mixed calcareous-siliceous oozes that characterize the apparently complete Oligocene/Miocene boundary interval at Site 959. These cycles suggest rhythmic fluctuations in local surface water fertility, perhaps associated with cyclic variations in upwelling intensity. These interbedded siliceous and mixed biogenic strata also provide an excellent opportunity to directly correlate silicoflagellate and calcareous nannofossil biostratigraphies for the tropical Atlantic. Shipboard work has indicated that significant problems exist in applying tropical lower Miocene correlations, largely established in the eastern equatorial Pacific, to the succession in the eastern tropical Atlantic.

The abundance of biosiliceous sedimentation in sediments at Site 959 suggests that these nutrient-rich waters were upwelling along the African margin throughout the Oligocene and early Miocene. However, this "silica" event is not unique to the eastern tropical Atlantic, as biosiliceous sediments are characteristic of Oligocene sections throughout the tropical Atlantic and both the Indian and Southern Atlantic sectors of the Southern Ocean (e.g., Barker, Kennett, et al., 1990; Ciesielski, Kristoffersen, et al., 1988; Schlich, Wise, et al., 1989; Wise, Schlich, et al., 1992; Baldauf and Barron, 1990; Curry, Shackleton, Richter, et al., 1995). The concentration of siliceous sedimentation has been used to infer that the most nutrient-enriched waters in the world ocean were in the Atlantic and that the modern deep-water "conveyor," flowing from the North Atlantic into the Pacific, was reversed relative to today (e.g., Wright et al., 1992). Hence, both

increased preservation within silica-enriched deep water and increased production in nutrient-enriched upwelled waters are probably responsible for the great abundance of these sediments on the West African Margin.

Biosiliceous sedimentation continued into the late early Miocene at Sites 959–962. Particularly noticeable is the preservation of siliceous deposits at Site 962, the deepest site. A similar episode of opal preservation is present in lower Miocene sections on the Ceara Rise in the western equatorial Atlantic and suggests widespread penetration of nutrient-rich deep waters into the tropical Atlantic (e.g., Curry, Shackleton, Richter, et al., 1995). The peak in late early Miocene silica sedimentation at Site 962 is more than twice the total sedimentation rate at shallower sites such as Site 960, and greater by one-third than the sedimentation rate at Site 959. Increased sedimentation rates at Site 962 relative to shallower sites suggest that differential preservation of opal may be responsible. All sites lie under the same surface water mass and are within 10 km of each other. Hence, it is reasonable to assume that production rates in the overlying waters were similar. We infer that Site 962 was bathed by nutrient-rich deep waters, whereas the intermediate waters covering Sites 959 and 960 may have been more corrosive to silica.

Middle Miocene "Carbonate Crisis"

The middle Miocene was characterized by low sediment accumulation rates (Site 959) or unconformities (Sites 960 and 962; Fig. 14), reflecting the middle Miocene carbonate crisis known from other oceans. At Site 959, sedimentation rates were lowest during the late middle Miocene between 11.5 and 13 Ma. This same time interval is represented by a hiatus at Sites 960 and 962. The middle Miocene is commonly represented by a hiatus throughout the world's oceans or as a period of low carbonate accumulation rates (e.g., Keller and Barron, 1983; Peterson et al., 1992). Peterson et al. (1992) attribute the middle Miocene "carbonate crisis" to a rise in the CCD, enhanced winnowing, and a drop in surface water productivity.

Evidence from Sites 959–962 supports both a change in CCD and current strength. Dissolution is intense even within the middle Miocene at Site 959 (water depth 2091 m), and no carbonate sediments are preserved at Site 962, the deepest site occupied. Apparently, corrosive waters were present up to intermediate depths in the eastern equatorial Atlantic. Good carbonate preservation is found for this period at sites of 2–3 km water depth in the western Atlantic and Caribbean (e.g., DSDP Site 151 and ODP Site 925). Hence, there appears to be an east-to-west asymmetry in carbonate preservation within intermediate waters in the tropical Atlantic. This asymmetry may reflect the penetration of relatively nutrient-enriched intermediate waters into the eastern basins of the Atlantic at the same time that young, nutrient-depleted, intermediate and deep waters flowed into the western basins. At the same time, intermediate water currents flowing along the west African coast may have increased in velocity. High current strengths are suggested by the absence of middle Miocene sediments on the topographic high drilled at Site 960, and their presence at Site 959 in the Deep Ivorian Basin, which is at nearly the same water depth.

Because of the widespread unconformities associated with the middle Miocene in all of the major ocean basins, the complete section at Site 959 has the potential to serve as an important biostratigraphic reference section for this part of the column in the eastern equatorial Atlantic.

The middle/late Miocene boundary corresponds approximately with an increase of carbonate sediment accumulation rates at Site 959, and was accompanied by an episode of carbonate accumulation at Site 960. Site 962 apparently remained well below the CCD throughout this time. A more significant change in sedimentation occurred after about 6.5 Ma, when accumulation rates rose sharply at Site 959, and to a lesser extent at Sites 960 and 961. The significant

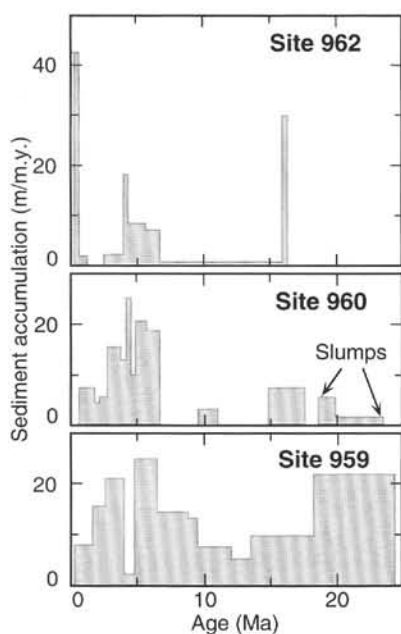


Figure 14. Diagram showing the variation in sedimentation rates at Sites 959, 960, and 962.

carbonate accumulation rate of 20 m/m.y. near the Marginal Ridge summit at Site 960, and the accumulation of significant pelagic clay on the slope of the Marginal Ridge at Site 962, indicate that intermediate and deeper water current velocities had decreased enough to allow accumulation at these relatively exposed sites. The timing of this pulse of increased accumulation rates corresponds to a similar pulse of carbonate accumulation in the equatorial Pacific and Indian oceans (Rio et al., 1990) in response to a brief (approximately 2 m.y.) deepening of the CCD. This event in the Atlantic has been related to an increase in the production of North Atlantic Deep Water (Berger, 1978; Larsen, Saunders, Clift, et al., 1994).

Pliocene

The enhanced rates of calcareous productivity and accumulation persisted across the Miocene/Pliocene boundary at both Sites 959 and 960. The late Miocene and early Pliocene were times of unusually high rates of carbonate accumulation throughout the tropical Indian, Atlantic, and western Pacific oceans. The presence of carbonate sediments of latest Miocene or early Pliocene age at Site 962 attests to the probable drop in the CCD in the eastern Atlantic at this time. Similar evidence for a depressed CCD comes from depth transects drilled in the Indian and Pacific oceans. These transects suggest that carbonate accumulation rates remained comparable between sites in intermediate water and upper deep water (Peterson et al., 1992).

The expanded sections across this boundary from Leg 159 should yield valuable data on the evolution of calcareous nannofossils including some groups, such as the ceratoliths and gephyrocapsids, that are important constituents of the coccolithophorid floras of the modern tropical oceans. Paleomagnetic records from these sites should provide additional control for calibrating an improved biostratigraphy for the eastern equatorial Atlantic throughout this interval.

Most of these regions also record a drop in mass accumulation rates between 4.5 and 2.0 Ma (e.g., Peterson et al., 1992). Sites 959–962 also have a condensed interval or hiatus that is centered around 2.0–2.5 Ma. This event may correlate with expansion of the Arctic ice cap and cooling events in North Atlantic Deep Water as suggested by Stein et al. (1986). Stein et al. (1986) suggest that high latitude cooling may have increased flow rates in both intermediate and deep waters and use this inference to explain the distribution of hiatuses in the northeastern Atlantic. This episode of reduced sediment accumulation at Sites 959–962 also coincides with a period of sediment drift migration in the North Atlantic (Kidd and Hill, 1986). The reduction of sedimentation rates at Site 959 and the formation of a hiatus at Site 962 may reflect a similar increase in winnowing by intermediate and deep waters off the West African Margin. The Pliocene–Pleistocene record from the three APC sites (959, 960, and 962) provides a complete composite record of the last 5.4 m.y. Shallower Sites 959 and 960 both contain nearly complete and continuous records of pelagic carbonate sedimentation through this time interval.

Significant changes in the ratio of the deep-living *Florisphaera profunda* vs. shallow-dwelling coccoliths occur throughout the upper Neogene of all sites drilled during Leg 159. The relative proportions of these taxa are known to respond to variations in the depth of the nutricline, with *F. profunda* being abundant where the nutricline is deep and the overlying surface water is clear (Molfino and McIntyre, 1990; Ahagon et al., 1993), whereas shallow-dwelling coccolithophorids are preferred under conditions of a shallow nutricline and/or turbid surface waters. High-resolution sampling of these sections will provide a detailed record of nutricline fluctuations during the Pliocene–Pleistocene.

SUMMARY

Drilling of the Côte d'Ivoire-Ghana Marginal Ridge represents the first scientific drilling survey of a transform passive margin and a

major advance in our understanding of the evolution of this type of margin beyond that already discovered through dredging or remote geophysical surveying techniques. Shipboard analyses document the evolution of an intracontinental pull-apart basin filled by lacustrine sediments, which was then transgressed by marine sediments as rifting progressed. Continuous shearing resulted in strong brittle deformation and soft sedimentary folding and slumping. Sometime between the Albian and the Turonian the pull-apart type basins underwent structural inversion and the Marginal Ridge was created as a topographic high on which shallow-water sediments were deposited.

Maximum uplift occurred between Turonian and late Santonian times when Sites 959 and 960, on the shallowest part of the Marginal Ridge, show evidence for the nearby presence of a high energy reef environment. This peak in uplift also correlates with the presumed time of migration of an oceanic spreading center along the southern edge of the transform margin. It is believed that the transfer of heat from this spreading ridge to the continental margin is responsible for the regional uplift of the Marginal Ridge. The passage of this spreading center marks the end of an active transform stage and the start of passive margin subsidence. Evidence for compression or strike-slip motion is not found for the period after this time, and the pre-Santonian sediments are all seen to be thermally more mature than younger sediments.

In the Late Cretaceous a thick sequence of organic-rich black shales accumulated in the Deep Ivorian Basin (Site 959), while the Marginal Ridge itself was eroded or accumulated current-winnowed hardgrounds. The Marginal Ridge may have acted as a sill to the Deep Ivorian Basin, and so promoted the poor circulation and deposition of organic-rich shales. A hiatus is seen to have affected much of the Paleocene at probably all the sites. The early Eocene was characterized by the start of porcellanite deposition in the Deep Ivorian Basin. Biosiliceous sedimentation spread to the Marginal Ridge shortly after this time, although the early Eocene was marked by deposition of a palygorskite-rich claystone. A deep-water depositional environment of this claystone is inferred from the microfauna, although typically palygorskite requires high salinities for its formation, most often found in very shallow evaporitic conditions. The palygorskite here may be redeposited or formed in the presence of deep-water brines. Biosiliceous sedimentation in the form of diatomite is seen in the Oligocene of Sites 959–961, although at Site 960 evidence suggests significant slumping and redeposition of this sediment off the crest of the Marginal Ridge at this time. Organic carbon contents of these sediments can be locally high, and a generally high nutrient level, possibly caused by upwelling, is inferred for the margin at that time. After the late early Miocene, deposition was dominated by a clayey nannofossil sediment, except at Site 962, which lies below the CCD and thus accumulated clays. Site 962 shows evidence for significant mass wasting and erosion of older (possibly Cretaceous) margin sediments during the Pliocene–Pleistocene, possibly related to low sea levels at that time.

REFERENCES

- Ahagon, N., Tanaka, Y., and Ujiie, H., 1993. *Florisphaera profunda*, a possible nannoplankton indicator of late Quaternary changes in sea-water turbidity at the northwestern margin of the Pacific. *Mar. Micropaleontol.*, 22:255–273.
- Baldauf, J.G., and Barron, J.A., 1990. The distribution of Eocene through Quaternary biosiliceous sediments: a distribution resulting in part from Polar cooling. In Bliel, U., and Thiede, J. (Eds.), *Geological History of the Polar Oceans: Arctic versus Antarctic*: Dordrecht (Kluwer), 575–607.
- Barker, P.F., Kennett, J.P., et al., 1990. *Proc. ODP. Sci. Results*, 113: College Station, TX (Ocean Drilling Program).
- Basile, C., Brun, J.P., and Mascle, J., 1992. Structure et formation de la marge transformante de Côte d'Ivoire-Ghana: apports de la sismique réflexion et de la modélisation analogique. *Bull. Soc. Geol. Fr.*, 163:207–216.

- Basile, C., Mascle, J., Popoff, M., Bouillin, J.P., and Mascle, G., 1993. The Côte d'Ivoire-Ghana transform margin: a marginal ridge structure deduced from seismic data. *Tectonophysics*, 222:1–19.
- Ben-Avraham, Z., Almagor, G., and Garfunkel, Z., 1979. Sediments and structure of the Gulf of Eilat (Aqaba)—northern Red Sea. *Sediment. Geol.*, 23:239–267.
- Berger, W.H., 1978. Sedimentation of deep-sea carbonate: maps and models of variations and fluctuations. *J. Foraminiferal Res.*, 8:286–302.
- Chamley, H., 1989. *Clay Sedimentology*: Berlin (Springer-Verlag).
- Chamley, H., and Debrabant, P., 1984. Mineralogical and geochemical investigations of sediments on the Mazagan Plateau, Northwestern African margin (Leg 79 Deep Sea Drilling Project). In Hinz, K., Winterer, E.L., et al., *Init. Repts. DSDP, 79*: Washington (U.S. Govt. Printing Office), 497–508.
- Ciesielski, P.F., Kristoffersen, Y., et al., 1988. *Proc. ODP, Init. Repts.*, 114: College Station, TX (Ocean Drilling Program).
- Crowell, J.C., 1974. Origin of late Cenozoic basins in southern California. In Dickinson, W.R. (Ed.), *Tectonics and Sedimentation*. Spec. Publ.—Soc. Econ. Paleontol. Mineral., 22:190–204.
- Curry, W.B., Shackleton, N.J., Richter, C., et al., 1995. *Proc. ODP, Init. Repts.*, 154: College Station, TX (Ocean Drilling Program).
- deMenocal, P.B., Ruddiman, W.F., and Pokras, E.M., 1993. Influence of high- and low-latitude on African terrestrial climate: Pleistocene eolian records from equatorial Atlantic Ocean Drilling Program Site 663. *Paleoceanography*, 8:209–242.
- Emerson, S., and Hedges, J.I., 1988. Processes controlling the organic carbon content of open ocean sediments. *Paleoceanography*, 3:621–634.
- Gradstein, F.M., and Berggren, W.A., 1981. Flysch-type agglutinated foraminifera and the Maastrichtian to Paleogene history of the Labrador and North seas. *Mar. Micropaleontol.*, 6:211–269.
- Jansa, L., Enos, P., Tucholke, B.E., Gradstein, F.M., and Sheridan, R.E., 1979. Mesozoic-Cenozoic sedimentary formations of the North American Basin, western North Atlantic. In Talwani, M., Hay, W., and Ryan, W.B.F. (Eds.) *Deep Drilling Results in the Atlantic Ocean: Continental Margins and Paleoenvironment*. Am. Geophys. Union, Maurice Ewing Ser., 3:1–57.
- Jones, B.F., and Galán, E., 1988. Sepiolite and palygorskite. In Bailey, S.W. (Ed.), *Hydrous Phyllosilicates (Exclusive of Micas)*. Rev. Mineral., 19:631–674.
- Kastner, M., 1981. Authigenic silicates in deep sea sediments: formation and diagenesis. In Emiliani, C. (Ed.), *The Sea (Vol. 7): The Oceanic Lithosphere*: New York (Wiley), 915–980.
- Keller, G., and Barron, J.A., 1983. Paleoceanographic implications of Miocene deep-sea hiatuses. *Geol. Soc. Am. Bull.*, 97:590–613.
- Kidd, R.B., and Hill, P.R., 1986. Sedimentation on mid-ocean sediment drifts. In Summerhayes, C.P., and Shackleton, N.J. (Eds.), *North Atlantic Paleoceanography*. Geol. Soc. Spec. Publ., 21:87–102.
- Larsen, H.C., Saunders, A.D., Clift, P.D., et al., 1994. *Proc. ODP, Init. Repts.*, 152: College Station, TX (Ocean Drilling Program).
- Mascle, J., and Blarez, E., 1987. Evidence for transform margin evolution from the Côte d'Ivoire-Ghana continental margin. *Nature*, 326:378–381.
- Mascle, J., Guiraud, M., Basile, C., Benkheilil, J., Bouillin, J.P., Cousin, M., and Mascle, G., 1993. La marge transformante de Côte d'Ivoire-Ghana: premiers résultats de la campagne Equanaute (Juin 1992). *C. R. Acad. Sci. Ser. 2*, 316:1255–1261.
- McKenzie, D.P., 1978. Some remarks on the development of sedimentary basins. *Earth Planet. Sci. Lett.*, 40:25–32.
- Molfino, B., and McIntyre, A., 1990. Nutricline variations in the equatorial Atlantic coincident with the Younger Dryas. *Paleoceanography*, 5:997–1008.
- Moore, D.M., and Reynolds, R.C., Jr., 1989. *X-ray Diffraction and the Identification and Analysis of Clay Minerals*: Oxford (Oxford Univ. Press).
- Odin, G.S., and Matter, A., 1981. De glauconiarum origine. *Sedimentology*, 28:611–641.
- Peterson, L.C., Murray, D.W., Ehrmann, W.U., and Hempel, P., 1992. Cenozoic carbonate accumulation and compensation depth changes in the Indian Ocean. In Duncan, R.A., Rea, D.K., Kidd, R.B., von Rad, U., and Weissel, J.K. (Eds.), *Synthesis of Results from Scientific Drilling in the Indian Ocean*. Geophys. Monogr., Am. Geophys. Union, 70:311–333.
- Pitman, W.C., and Andrews, J.A., 1985. Subsidence and thermal history of small pull-apart basins. In Biddle, K.T., and Christie-Blick, N. (Eds.), *Strike-slip Deformation, Basin Formation, and Sedimentation*. Spec. Publ.—Soc. Econ. Paleontol. Mineral., 37:45–49.
- Rio, D., Fornaciari, E., and Raffi, I., 1990. Late Oligocene through early Pleistocene calcareous nannofossils from western equatorial Indian Ocean (Leg 115). In Duncan, R.A., Backman, J., Peterson, L.C., et al., *Proc. ODP, Sci. Results*, 115: College Station, TX (Ocean Drilling Program), 175–235.
- Ruddiman, W.F., and Janacek, T.R., 1989. Pliocene-Pleistocene biogenic and terrigenous fluxes at equatorial Atlantic Sites 662, 663, and 664. In Ruddiman, W., Sarnthein, M., et al., *Proc. ODP, Sci. Results*, 108: College Station, TX (Ocean Drilling Program), 211–240.
- Sarnthein, M., Winn, K., Duplessy, J.-C., and Fontugne, M.R., 1988. Global variations of surface ocean productivity in low and mid latitudes: influence on CO₂ reservoirs of the deep ocean and atmosphere during the last 21,000 years. *Paleoceanography*, 3:361–399.
- Schlich, R., Wise, S.W., Jr., et al., 1989. *Proc. ODP, Init. Repts.*, 120: College Station, TX (Ocean Drilling Program).
- Singer, A., 1979. Palygorskite in sediments: detrital, diagenetic or neoformed: a critical review. *Geol. Rundsch.*, 68:996–1008.
- Stein, R., Sarnthein, M., and Suendermann, J., 1986. Late Neogene submarine erosion events along the north-east Atlantic continental margin. In Summerhayes, C.P., and Shackleton, N.J. (Eds.), *North Atlantic Paleoceanography*. Geol. Soc. Spec. Publ., 21:103–118.
- Stein, R., Littke, R., Stax, R., and Welte, D.H., 1989. Quantity, provenance, and maturity of organic matter at ODP Sites 645, 646, and 647: implications for reconstruction of paleoenvironments in Baffin Bay and Labrador Sea during Tertiary and Quaternary time. In Srivastava, S.P., Arthur, M.A., Clement, B., et al., *Proc. ODP, Sci. Results*, 105: College Station, TX (Ocean Drilling Program), 185–208.
- Thiry, M., and Jacquin, T., 1993. Clay mineral distribution related to rift activity, sea-level changes and paleoceanography in the Cretaceous of the Atlantic Ocean. *Clay Miner.*, 28:61–84.
- Tiedemann, R., Sarnthein, M., and Stein, R., 1989. Climatic changes in the western Sahara: aeolo-marine sediment record of the last 8 million years (Sites 657–661). In Ruddiman, W., Sarnthein, M., et al., *Proc. ODP, Sci. Results*, 108: College Station, TX (Ocean Drilling Program), 241–277.
- Verardo, D.J., and McIntyre, A., 1994. Production and destruction: control of biogenous sedimentation in the tropical Atlantic 0–300,000 years B.P. *Paleoceanography*, 9:63–86.
- Watkins, D.K., Erba, E., and Premoli Silva, I., in press. Cretaceous and Paleogene manganese-encrusted hardgrounds from central Pacific guyots. *Proc. Sci. Results*, 144.
- Weaver, C.E., 1989. *Clays, Muds, and Shales*: New York (Elsevier), Dev. Sedimentol., 44.
- Wise, S.W., Jr., Schlich, R., et al., 1992. *Proc. ODP, Sci. Results*, 120 (Pts. 1 and 2): College Station, TX (Ocean Drilling Program).
- Wolfart, R., 1982. Cretaceous radiolaria from the Northwest African Continental Margin. In von Rad, U., Hinz, K., Sarnthein, M., and Seibold, E. (Eds.), *Geology of the Northwest African Continental Margin*: Berlin (Springer), 354–365.
- Wright, J.D., Miller, K.G., and Fairbanks, R.G., 1992. Early and middle Miocene stable isotopes: implications for deep-water circulation and climate. *Paleoceanography*, 7:357–389.

Ms 159IR-109